Differential Regulation of Vascular Tone and Remodeling via Stimulation of Type 2 and Type 6 Adenylyl Cyclases in the Ductus Arteriosus

Utako Yokoyama, Susumu Minamisawa, Ayako Katayama, Tong Tang, Sayaka Suzuki, Kousaku Iwatsubo, Shiho Iwasaki, Reiko Kurotani, Satoshi Okumura, Motohiko Sato, Shumpei Yokota, H. Kirk Hammond, Yoshihiro Ishikawa

Rationale: Prostaglandin (PG)E_2, which increases intracellular cAMP via activation of adenylyl cyclases (ACs), induces vasodilation and hyaluronan-mediated intimal thickening (IT) in the ductus arteriosus (DA) during late gestation. After birth, however, differential regulation of vasodilation and IT is preferable for treatment of patients with patent DA and DA-dependent congenital cardiac malformations.

Objective: Our objectives were to examine whether AC isoforms play differential roles in DA vasodilation and IT.

Methods and Results: AC2 and AC6 were more highly expressed in rat DA than in the aorta during the perinatal period. AC6-targeted siRNA counteracted PGE_1-induced hyaluronan production in rat DA smooth muscle cells. Overexpression of AC6 enhanced PGE_1-induced hyaluronan production and induced IT in DA explants. Furthermore, IT of the DA was less marked in mice lacking AC6 than in wild-type and AC5-deficient mice. Stimulation of AC2 attenuated AC6-induced hyaluronan production via inhibition of the p38 mitogen-activated protein kinase pathway and AC6-induced IT of the DA. An AC2/6 activator, 6-[*N*-(2-isothiocyanatoethyl) aminocarbonyl] forskolin (FD1), did not induce hyaluronan-mediated IT in DA explants, although an AC5/6 activator, 6-[3-(dimethylamino)propionyl]-14,15-dihydroforskolin (FD6) did. Moreover, FD1 induced longer vasodilation of the DA than did PGE_1 without significant adverse effects in vivo.

Conclusions: AC6 is responsible for hyaluronan-mediated IT of the DA and AC2 inhibited AC6-induced hyaluronan production. Stimulation of both AC2 and AC6 by FD1 induced longer vasodilation without hyaluronan-mediated IT in the DA in vivo. FD1 may be a novel alternative therapy to currently available PGE therapy for patients with DA-dependent congenital heart disease. (*Circ Res.* 2010;106:1882-1892.)

Key Words: patent ductus arteriosus ■ prostaglandins ■ smooth muscle ■ vasodilation ■ remodeling

Prostaglandin (PG)E_2 and PGE_1 play principal roles in maintaining the patency of the ductus arteriosus (DA) during gestation. PGE_1 is widely used to keep the DA open in patients with DA-dependent congenital heart diseases, because both PGE_1 and PGE_2 increase the intracellular concentration of cAMP, resulting in vasodilation in the DA.[1,2] On the other hand, we have demonstrated that PGE-EP4-cAMP signals during late gestation increased hyaluronan production in the DA and consequently induced intimal thickening (IT), which is critical for permanent closure of the DA after birth.[3] Therefore, the effects of $PGE_{1/2}$ on vasodilation and remodeling oppose each other in terms of regulation of the DA after birth. Differential regulation of vasodilation and IT in the DA would be preferable for patients who need PGE/anti-PGE therapy.

Because intracellular cAMP is synthesized by adenylyl cyclases (ACs), which are transmembrane enzymes activated by G protein-coupled receptors, including PGE receptors, ACs must play an important role in regulating vasodilation and remodeling in the DA. To date, nine different isoforms of membrane-bound forms of ACs (AC1 through AC9) have been identified in vertebrate tissues.[4] Most tissues express several AC isoforms, which exhibit remarkable diversities in their biochemical properties.[5,6] Because smooth muscle cells

Original received December 13, 2009; revision received April 12, 2010; accepted April 15, 2010.

From the Cardiovascular Research Institute (U.Y., A.K., S.S., R.K., S.O., M.S., Y.I.), the Department of Pediatrics (S.I., S.Y.), Yokohama City University Graduate School of Medicine, Japan; the Department of Life Science and Medical Bioscience (S.M.), Waseda University Graduate School of Advanced Science and Engineering, Tokyo, Japan; VA San Diego Healthcare System (T.T., H.K.H.), San Diego, Calif; the Department of Medicine (T.T., H.K.H.), University of California San Diego, La Jolla; the Cardiovascular Research Institute, Departments of Cell Biology & Molecular Medicine and Medicine (Cardiology) (K.I.,Y.I.), New Jersey Medical School, University of Medicine & Dentistry of New Jersey, Newark.

Correspondence to Susumu Minamisawa, Department of Life Science and Medical Bioscience, Waseda University Graduate School of Advanced Science and Engineering, 2-2, Wakamatsu-cho, TWIns, Shinjuku-ku, Tokyo 162-8480, Japan (E-mail sminamis@waseda.jp); or to Yoshihiro Ishikawa, the Cardiovascular Research Institute, Yokohama City University Graduate School of Medical Science, Yokohama 236-0004, Japan (E-mail yishikaw@yokohama-cu.ac.jp).

Circulation Research **is available at http://circres.ahajournals.org** **DOI: 10.1161/CIRCRESAHA.109.214924**

(SMCs) in the DA exert biological properties distinct from SMCs in other vessels such as the aorta, we hypothesized that such properties are attributable, at least in part, to the distinct roles of specific AC isoforms in the DA.

In addition to the role of $PGE_{1/2}$ in vasodilation, the PGE-AC-cAMP signal cascade has been shown to regulate vascular remodeling.[7,8] For example, cAMP markedly inhibits proliferation of SMCs[9] and reduces IT after arterial injury in vivo,[10] a process that shares many aspects with IT in the DA.[1,11] Interestingly, several studies have demonstrated that $PGE_{1/2}$ inhibits the proliferation of vascular SMCs,[7,8] whereas others have reported that PGE_2 stimulates the growth of vascular SMCs.[12,13] Such diversities in the effects of PGE signaling might be related to differential expression of AC isoforms among vascular tissues. It has been difficult, however, to evaluate the contribution of ACs to relevant phenomena in an AC isoform-dependent manner, because multiple isoforms of ACs are coexpressed. This is partially attributable to the lack of available AC isoform-selective pharmacological regulators. In previous studies, we synthesized more than 200 new derivatives of forskolin (a non–isoform-selective AC activator) and identified derivatives that are selective to specific AC isoforms.[6,14,15] Such AC isoform-selective activators enable us to explore the role of each AC isoform in vascular tone and remodeling especially in vivo. In the present study, using such AC isoform-specific activators, overexpression or selective silencing of AC isoforms and AC-isoform deficient-mice, we have investigated the role of AC isoforms and the availability of AC isoform-selective activators in regulating DA vascular tone and remodeling.

Non-standard Abbreviations and Acronyms

AC	adenylyl cyclase
Adv	adenovirus-mediated gene transfer
DA	ductus arteriosus
E	embryonic day
ERK	extracellular signal-related kinase
FD1	6-[*N*-(2-isothiocyanatoethyl) aminocarbonyl] forskolin
FD6	6-[3-(dimethylamino)propionyl]-14,15-dihydroforskolin
HAS2	hyaluronan synthase type 2
IT	intimal thickening
JNK	c-Jun N-terminal kinase
KO	knockout
MAPK	mitogen-activated protein kinase
PGE	prostaglandin E
PK	protein kinase
siRNA	small interfering RNA
SMC	smooth muscle cell

Methods

An expanded Methods section is available in the Online Data Supplement at http://circres.ahajournals.org.

Reagents

Forskolin derivatives: 6-[*N*-(2-isothiocyanatoethyl) aminocarbonyl] forskolin (FD1),[14,16] and 6-[3-(dimethylamino)propionyl]-14,15-dihydroforskolin (FD6)[14] were kindly provided by Nippon Kayaku Co, Ltd (Tokyo, Japan).

Animals and Tissues

All animals were cared for in compliance with the guiding principles of the American Physiological Society. The experiments were approved by the ethical committee of animal experiments at Yokohama City University School of Medicine. Wistar rat embryos were obtained from timed-pregnant mothers (Japan SLC Inc, Shizuoka, Japan). Pooled tissues of DA and aorta were obtained from rat embryos on embryonic day (E)19 (n>60) and E21 (n>60) and neonates on the day of birth (day0, n>60). Generation and phenotypes of AC5 knockout mice (AC5KO) and AC6 knockout mice (AC6KO) have been described previously.[17,18] All mice were littermates from heterozygote crosses.

Isolation and Culture of Rat Ductus Arteriosus Smooth Muscle Cells

Vascular SMCs were obtained from DA and aorta of Wistar rat embryos at E21 as previously described.[19]

Quantitative and Semiquantitative RT-PCR

Isolation of total RNA and generation of cDNA were performed and RT-PCR analysis was done as previously described.[19] The primers were designed based on the rat nucleotide sequences of AC isoforms. Each primer set was designed between multiple exons (Online Table I), and PCR products were confirmed by sequencing. The abundance of each gene was determined relative to the GAPDH transcript using TaqMan Rodent GAPDH control reagents kits (Applied Biosystems, Foster City, Calif).

Immunoblot Analysis

Proteins from whole cells were analyzed by immunoblotting as previously described.[19]

RNA Interference

Double-stranded small interfering (si)RNAs to the selected regions of AC2–7 and the negative siRNA used as a control were purchased from QIAGEN (Hilden, Germany) or Invitrogen (San Diego, Calif) (Online Table II). According to the instructions of the manufacturer, cells were transfected with siRNA (300 pmol), using Lipofectamin RNAiMAX (Invitrogen).

Adenovirus Construction

Full-length cDNA-encoding rat AC2 was cloned into the shuttle vector for construction of an adenoviral vector harboring AC2 through the use of an AdenoX adenovirus construction kit (Clontech, Tokyo, Japan). Adenovirus encoding murine AC6 driven by a cytomegalovirus promoter was generated by homologous recombination as previously described.[20] Adenovirus encoding MKK3 was kindly provided by Dr Yibin Wang (University of California, Los Angeles).[21]

cAMP Production by Radioimmunoassay

Rat ductus arteriosus smooth muscle cells (DASMCs) were serum-starved for 48 hour and assayed for cAMP production by RIA after incubation with drugs of interest (Online Data Supplement).

Quantitation of Hyaluronan

The amount of hyaluronan in the cell culture supernatant was measured by the latex agglutination method as previously described.[3]

Organ Culture

DA organ culture was performed as previously described.[3,22]

Measurement of Isometric Tension of the Vascular Rings of DA

Isometric tension of the vascular rings of DA was measured as previously described.[23]

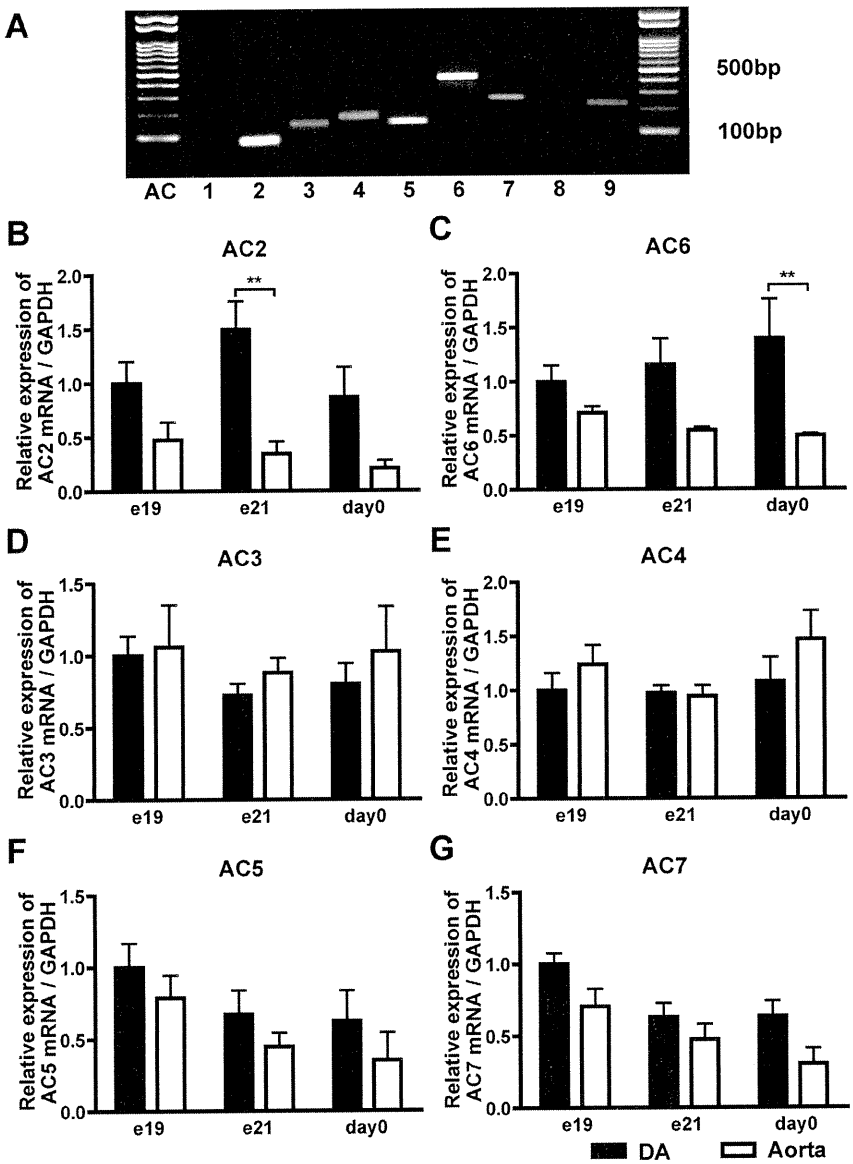

Figure 1. Multiple transcripts of AC isoforms in rat DA. A, mRNA expression of AC isoforms using semiquantitative RT-PCR in rat E21 DA. **B through G,** Quantitative RT-PCR analyses of AC2–7. $^{**}P<0.01$. Data are from 6 independent experiments.

Rapid Whole-Body Freezing Method

To study the in situ morphology and inner diameter of neonatal DA, a rapid whole-body freezing method was used as previously described.[24] The fetuses at E21 were delivered by cesarean section and intraperitoneally injected 1 hour after birth with PGE_1, FD1 or FD6 in 200 μL of saline. The minimal dose of FD1 (10.8 mg/kg of body weight) and FD6 (1.29 mg/kg of body weight) that caused maximal dilation in the DA were used.

Protein Kinase A Activity

Protein kinase (PK)A activity was measured using an assay kit (StressGen Biotechnologies, Ann Arbor, Mich) according to the instructions of the manufacturer, as described previously.[25]

Statistical Analysis

Data are shown as the means±SEM of independent experiments. Statistical analysis was performed between two groups by unpaired Student t test or between multi-groups by one-way ANOVA followed by Student–Newman–Keuls multiple comparison test. A value of $P<0.05$ was considered significant.

Results

Multiple Transcripts of AC Isoforms in Rat DA

First, we detected all isoforms except for AC1 and AC8 in rat E21 DA by semiquantitative analyses (Figure 1A). Next, quantitative RT-PCR analyses of AC2–7 showed that AC2, AC5, and AC6 were abundantly expressed in rat DA and that the expression levels of AC2 and AC6 were significantly higher in the DA than in the aorta during the perinatal period, whereas those of AC5 were comparable between the DA and the aorta. The expression of AC2 reached maximal level in E21 DA (Figure 1B), whereas that of AC6 was increased during development in rat DA (Figure 1C).

AC6 Is Responsible for Hyaluronan Production in DASMCs

We examined the contribution of AC2, AC5 and AC6 to PGE_1-induced cAMP production in DASMCs by using AC2-,

AC5-, and AC6-targeted siRNAs. The expression levels of ACs mRNAs using the siRNAs are shown in Online Figure I. Silencing of AC5 or AC6 dramatically decreased PGE_1-induced cAMP production and that of AC2 also decreased PGE_1-induced cAMP production by 58% (Figure 2A), indicating that AC2, AC5 and AC6 are major isoforms responsible for cAMP production by PGE_1 in DASMCs. We then examined the effect of ACs on hyaluronan production in DASMCs. AC6-targeted siRNA weakened PGE_1-induced hyaluronan production, whereas AC2-, and AC5-targeted siRNA did not (Figure 2B). Neither AC3-, AC4-, nor AC7-targeted siRNA weakened PGE_1-induced hyaluronan production (Online Figure II). Using adenovirus-mediated gene transfer of AC2 and AC6 (Adv.AC2 and Adv.AC6), efficacy of which is shown in Online Figure III, we found that the overexpression of AC6, but not of AC2, further enhanced PGE_1-induced hyaluronan production when compared with the overexpression of LacZ as a control (Figure 2C). Interestingly, co-overexpression of both AC2 and AC6 negated AC6-mediated enhancement of hyaluronan production.

AC6 Gene Transfer, but Not AC2, Promoted IT in Rat DA Explants

When AC6 was overexpressed in immature rat DA explants in which IT had not yet formed, prominent IT with strong hyaluronan deposition was observed in AC6-overexpressed DA explants, as compared to LacZ controls (Figure 3A, 3B, and 3D). The internal lumen of the DA treated with Adv.AC6 was almost completely closed (Figure 3C). However, overexpression of AC2 did not promote hyaluronan deposition and IT formation. Further, Adv.AC2 abrogated AC6 overexpression-induced hyaluronan production and IT ex vivo, which is consistent with the data in Figure 2C. Taken together, these results indicate that AC2 has an inhibitory effect on AC6-induced hyaluronan-mediated IT in DA explants.

AC6 Deficiency Decreased IT in Mouse DA

Although AC5 and AC6 share an extremely high amino acid homology, the above experiments suggested that AC6 is a major isoform for DA remodeling. We therefore examined whether AC6 indeed plays a major role in in vivo IT of the DA and found that genetic disruption of the AC6 isoform resulted in less IT during late gestation (E18.5) (Figure 4B, 4D, and 4F). It should be noted that DAs closed after birth in AC6KO mice (data not shown). The IT of AC5KO mice was normally developed at E18.5 (Figure 4A, 4C, and 4E), and the DA of AC5KO mice closed after birth (data not shown). These findings support the conclusion that AC6 plays a primary role in IT and, thus, the vascular remodeling in the mouse DA.

Effect of Isoform-Selective AC Activators on cAMP Accumulation in Rat DASMCs

Based on the findings of previous crystallographic studies and computer-assisted drug design, we identified forskolin derivatives (FD1 or FD6) that have enhanced selectivity for AC2 or AC5 in regulating tissue AC catalytic activity.[14]

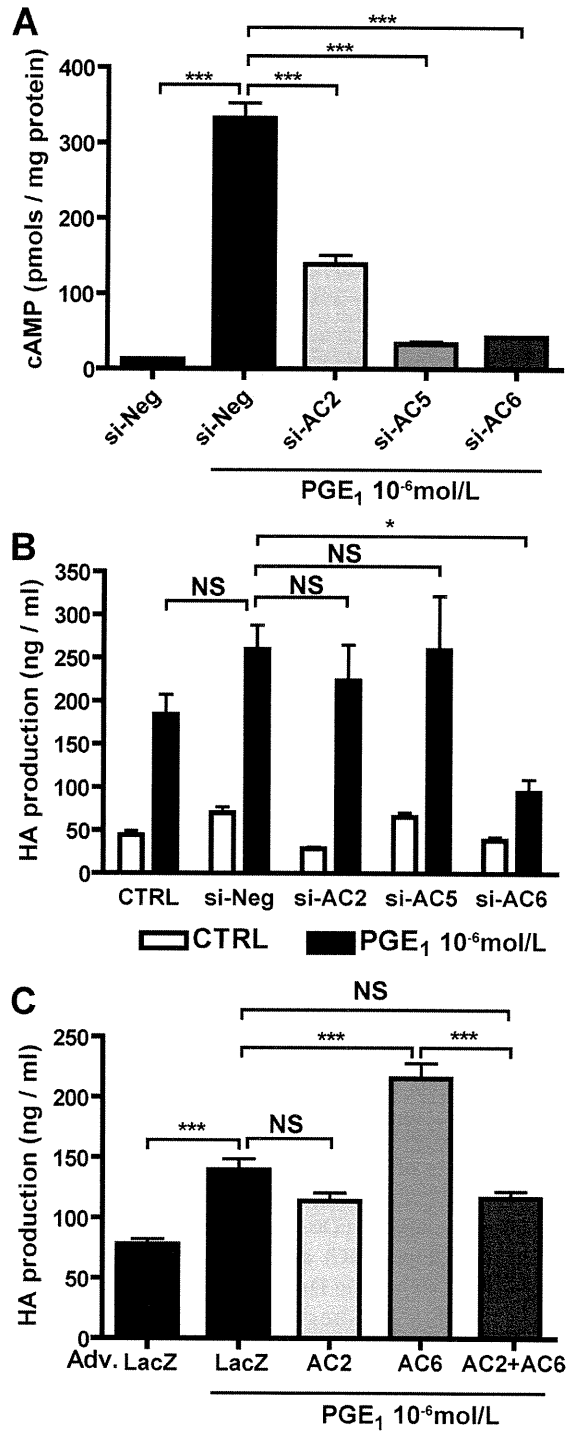

Figure 2. AC6 is responsible for hyaluronan production in DASMCs. A, PGE_1 induced cAMP accumulation in DASMCs in the cells treated with negative siRNA. AC2-, AC5-, and AC6-targeted siRNA decreased PGE_1-induced cAMP production (n=4). **B,** AC6-targeted siRNA attenuated PGE_1-induced hyaluronan (HA) production, whereas AC2- and AC5-targeted siRNA did not (n=7 to 11). **C,** Adv.AC6 enhanced PGE_1-induced hyaluronan production. Adv.AC2 abolished the Adv.AC6-induced enhancement of hyaluronan production (n=4). $^*P<0.05$ and $^{***}P<0.001$. NS indicates not significant.

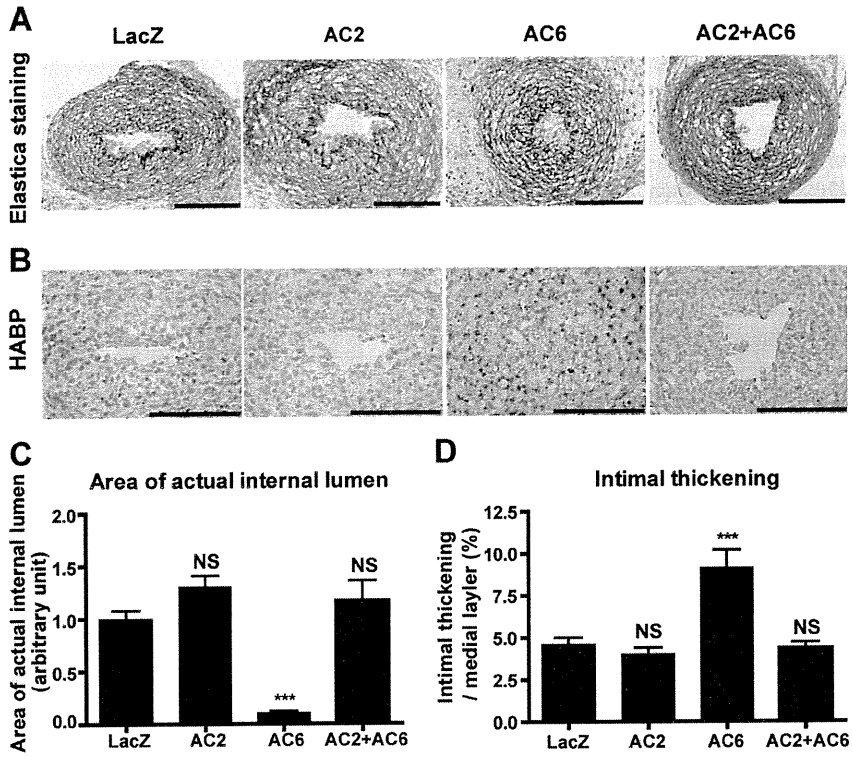

Figure 3. Adenovirus-mediated AC6 gene transfer promoted IT in rat DA explants. A, Elastica van Gieson staining for cultured DA explants overexpressed with Adv.LacZ, Adv.AC2, Adv.AC6, or Adv.AC2+Adv.AC6. **B,** Strong immunoreaction to hyaluronan in DA explants cultured with Adv.AC6. **Bars:** 100 μm. **C,** The area of the internal lumen of the DA treated with Adv.AC6 was significantly decreased (n=8 to 9). **D,** The ratio of IT to the thickness of the medial layer was increased in the DA treated with Adv.AC6, but not with Adv.AC2 (n=8 to 9). ***$P<0.001$. HABP indicates hyaluronan-binding protein.

However, the ability of cAMP production via AC6 of FD1 and FD6 has not been demonstrated. FD1 enhanced LacZ control-induced cAMP accumulation in DASMCs infected with Adv.AC2 or Adv.AC6 (Figure 5A). FD6 enhanced cAMP accumulation in DASMCs with Adv.AC6, but not with Adv.AC2. These data suggest that FD1 stimulates both AC2 and AC6 and that FD6 stimulates AC5 and AC6. We confirmed that FD1 (AC2/6 stimulator) and FD6 (AC5/6 stimulator) increased cAMP accumulation in DASMCs in a dose-dependent manner (Figure 5B).

The Effects of Isoform-Selective AC Activators on DASMC Hyaluronan Production

We then found that FD6 significantly increased hyaluronan production (Figure 5C) and transcripts of hyaluronan synthase type 2 (HAS2) in DASMCs at 10^{-5} mol/L (Figure 5D). In contrast, FD1, in doses up to $10^{-5.5}$ mol/L, did not increase hyaluronan production or HAS2 transcripts up. It should be noted that production of cAMP by FD1 at a concentration of $10^{-5.5}$ mol/L was equivalent to that by FD6 at 10^{-5} mol/L (Figure 5B and 5C) and that FD1 significantly decreased DASMC viability at a concentration higher than 10^{-5} mol/L. Silencing of AC6, but not of AC5, abolished FD6-induced hyaluronan production (Figure 5E), indicating that AC6 is responsible for FD6-induced hyaluronan production. Furthermore, to examine whether the effect of FD6 on hyaluronan production is specific to DASMCs, we found that FD6 did not induce hyaluronan production in SMCs from the rat aorta (Figure 5F), because expression of AC6 mRNA in aortic SMCs was approximately 60% lower than in DASMCs. However, when AC6 was overexpressed in the aortic SMCs, hyaluronan production was significantly increased by 1.4±0.1-fold (n=6) in the presence of FD6 (10^{-5} mol/L), suggesting that this data can provide insight into a more general vascular remodeling by AC6.

Involvement of MKK3-p38 MAPK in AC6-Induced Hyaluronan Production

To examine the mechanism by which AC2 inhibits AC6-induced hyaluronan production, we focused on several signal pathways such as p38 mitogen-activated protein kinase (MAPK). We found that FD6 increased phosphorylation of p38 protein in DASMCs, whereas FD1 and N6-Benzoyladenosine-cAMP (Bnz-cAMP), a PKA selective cAMP analog, did not (Figure 6A and 6B). FD6-induced phosphorylation of p38 and MKK3/6 was negated in DASMCs treated with AC6-targeted siRNA (Figure 6C). FD1 increased phosphorylation of p38 and MKK3/6 when AC2 expression was downregulated by AC2-targeted siRNA (Figure 6C). FD6-induced hyaluronan production was attenuated by SB203580, a p38 inhibitor, or H89, a PKA inhibitor. Combined treatment of SB203580 and H89 further inhibited hyaluronan production (Figure 6D). In contrast, SB203580 did not affect PKA-induced hyaluronan production (Figure 6E). These data suggest that p38 MAPK and PKA independently regulate hyaluronan production. Furthermore, overexpression of MKK3, the efficacy of which is demonstrated by Adv.MKK3 (Figure 6F), enhanced FD6-induced hyaluronan production in DASMCs (Figure 6G). Extracellular signal-related kinase (ERK)1/2 and c-Jun N-terminal kinase (JNK) were not phosphorylated by FD6 (data not shown). Phospholipase C, PKC, IP3 receptor, PI3-kinase, and Epac signaling were not

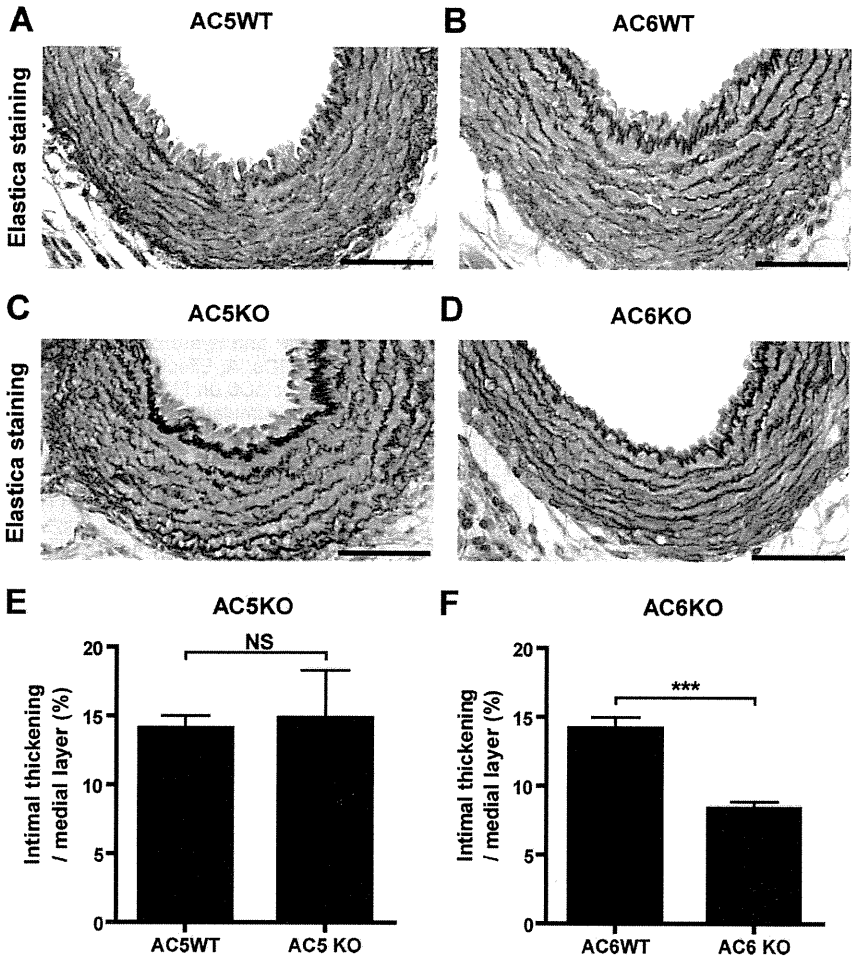

Figure 4. Impaired IT in the mouse DA attributable to AC6, but not AC5, deficiency. A, C, and E, DAs from AC5KO mice at E18.5 were stained with elastica van Gieson stain. Both AC5KO and wild-type (WT) mice showed IT in the DA (n=4 to 5). **B, D, and F,** DAs from AC6KO mice at E18.5 had less IT compared to wild-type mice (n=8). **Bars:** 50 μm. ***$P<0.001$.

involved in AC6-induced hyaluronan production, as shown using specific agonists or inhibitors for each pathway (Online Figure IV). These data indicate that stimulation of AC6 promotes hyaluronan production via both p38 and PKA pathways and that AC2 inhibits the AC6-activated MKK3-p38 pathway.

The Effects of Isoform-Selective AC Activators on IT Ex Vivo

We then examined the effects on FD1 and FD6 on IT using DA explants. Consistent with other data (Figures 5 and 6), 48 hour incubation with FD6 significantly induced IT, increased hyaluronan production, and narrowed the internal lumen in DA explants (Figure 7). It should be noted that FD1 and FD6, similarly to forskolin and PGE_1, inhibited proliferation of DASMCs. Overexpression of AC2 or AC6 also inhibited DNA synthesis in DASMCs (Online Figure V), indicating that FD6 does not directly promote IT by proliferation of DASMCs.

The Effects of Isoform-Selective AC Activators on Vasodilation

Because $PGE_{1/2}$ strongly dilates the DA via activation of ACs, AC activators should be potent vasodilators for the DA as well. We found that FD1 and FD6 similarly attenuated indomethacin-induced contraction in DA explants (Figure 8A). We then examined the vasodilatory effect of FD1 and FD6 in vivo using a whole-body freezing method. Here, the DA closed completely 1 hour after birth (Figure 8B) when PGE_1, FD1, or FD6 were administrated by intraperitoneal injection. Consistent with previous data,[24] PGE_1 caused maximal dilatation 30 minutes after injection and then the DA completely closed within 2 hour (Figure 8C and 8D). FD1 induced maximal dilatation of the DA up to 4 hour and then the DA gradually contracted, suggesting that FD1 has a longer vasodilatory effect on the DA than dose PGE_1. Although FD6 also dilated the DA 30 minutes after injection, all neonates died approximately 4 hours after injection because of suppression of respiration, which is the same side effect caused by PGE_1 and was not caused by FD1. We also found that FD1 and FD6 did not affect the diameter of the ascending aorta, whereas FD6, but not FD1, significantly dilated the main pulmonary artery up to 4 hour after administration (Online Figure VI, A through C). Using cultured DASMCs, AC6-targeted siRNA attenuated forskolin-induced phosphorylation of vasodilator-stimulated phosphoprotein (VASP), whereas AC2-targeted siRNA had no effect, suggesting that AC6 is primarily involved in DA vasodilation (Online Figure VI, D).

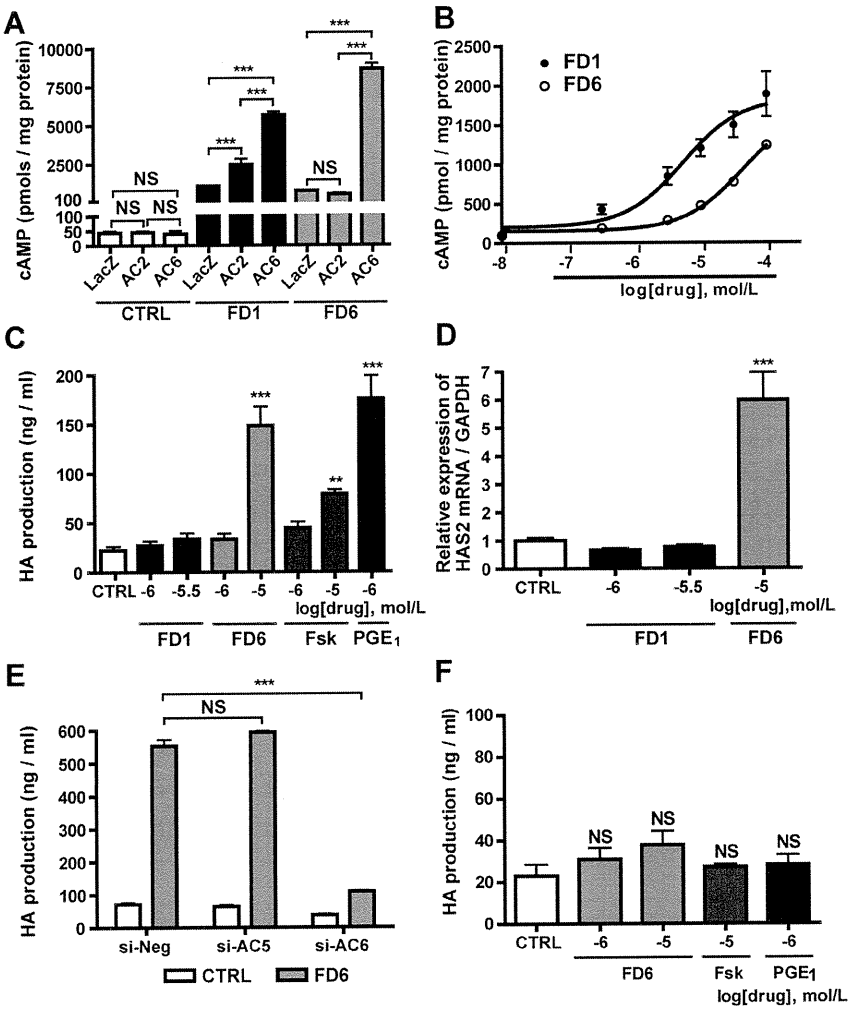

Figure 5. The effects of FD1 and FD6 on cAMP and hyaluronan production in DASMCs. A, Effect of overexpression of AC2 or AC6 on FD1- or FD6-induced cAMP accumulation (n=6). **B,** FD1 and FD6 increased cAMP accumulation in DASMCs in a dose-dependent manner (n=4). **C,** FD6, but not FD1, increased hyaluronan production (n=8 to 11). **D,** FD6 significantly increased HAS2 mRNA (n=6). **E,** AC6-targeted siRNA negated FD6-induced hyaluronan production (n=4). **F,** FD6, PGE_1, and forskolin did not induce hyaluronan production in aortic SMCs (n=6). $^{**}P<0.01$ and $^{***}P<0.001$ vs control (CTRL). Fsk indicates forskolin.

Taken together, these results reveal that AC6 play a primary role in hyaluronan-mediated vascular remodeling in the DA through activation of the PKA and MKK3-p38 MAPK pathways and that AC2 has an inhibitory effect on AC6-mediated hyaluronan production and IT.

Discussion

The Effect of AC2, AC5, and AC6 on Vascular Remodeling

The present study demonstrated for the first time that AC plays a significant role in vascular remodeling in the DA. Intimal thickening during development is a critical form of vascular remodeling for postnatal closure of the DA.[3,26] We found that hyaluronan induced by PGE-EP4-cAMP signaling is a prominent constituent of the extracellular matrix of IT in the DA.[3] It seems a worthwhile endeavor to investigate mechanisms leading to an increase in hyaluronan, because insights into its regulatory mechanisms and signaling pathways might eventually lead to ways of controlling hyaluronan-mediated IT in the DA. However, the isoform-selective role of AC in DA vascular remodeling has not previously been reported. Importantly, we found that AC6 is responsible for hyaluronan-mediated IT in the DA via activation of the MKK3-p38 and PKA pathways and that AC2 has an inhibitory effect on AC6-mediated hyaluronan production and DA remodeling. We also demonstrated that simultaneous stimulation of AC2 and AC6 by FD1 produces a longer vasodilatory effect than does PGE_1 without inducing hyaluronan-mediated IT.

It is important to identify whether the source of hyaluronan is from SMCs or endothelial cells of the DA. Using cell sorting analysis, we found that the expression levels of HAS1, HAS2 and AC6 mRNAs in CD31-positive/CD45-negative endothelial cells from E21 rat DA were significantly lower than those in CD31-negative/CD45-negative SMCs from E21 rat DA (Online Figure VII). Therefore, we believe that DASMCs are a major source of hyaluronan production.

DA IT in AC6-Deficient Mice

Our results also showed that the DA of AC6KO mice had less fully formed IT during late gestation. These results support the belief that AC6 plays a role in EP4-mediated hyaluronan synthesis. Nevertheless, the DA of AC6KO mice eventually closed after birth, similarly to wild-type mice, whereas the DA remained open in EP4KO mice. These results suggest

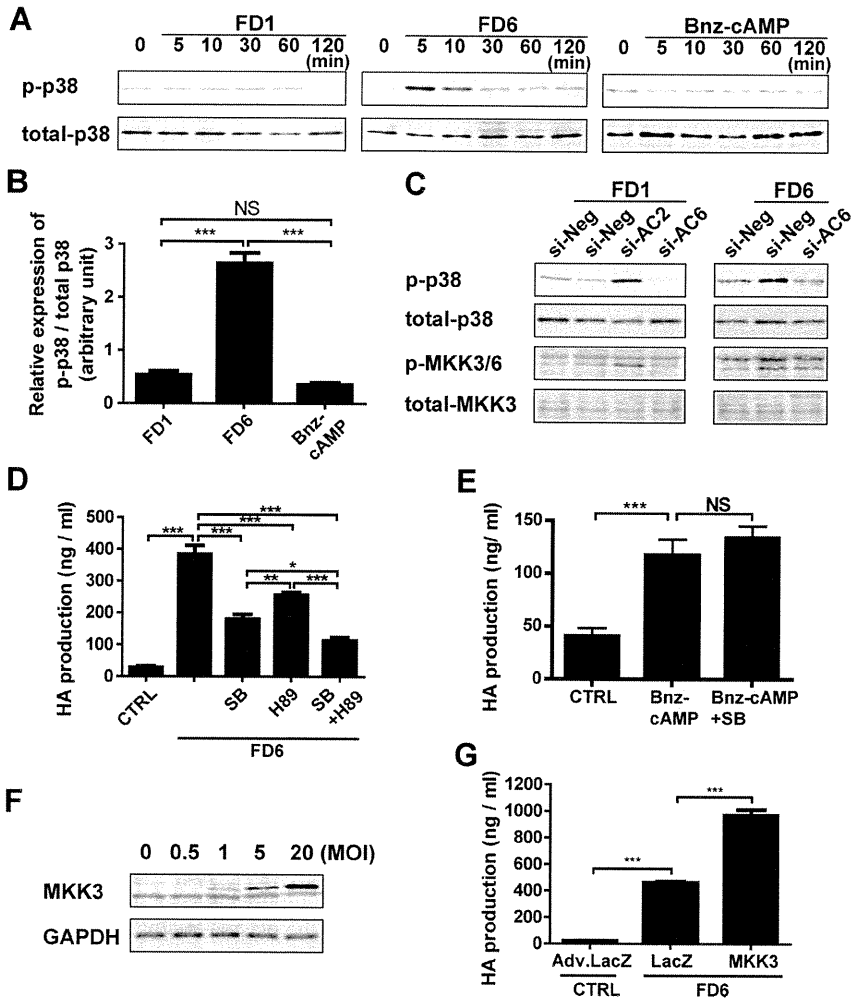

Figure 6. The signaling pathway of AC6-induced hyaluronan production in DASMC. A, Phosphorylation of p38 protein (p-p38) by FD1 ($10^{-5.5}$ mol/L), FD6 (10^{-5} mol/L), or Bnz-cAMP (10^{-5} mol/L) (n=4). **B,** Quantification of the ratio of p-p38 to total p38 after 5 minutes stimulation by FD1, FD6 or BnzcAMP. (n=4). **C,** Phosphorylation of p38 and MKK3/6 induced by 5 minutes treatment of FD1 ($10^{-5.5}$ mol/L) or FD6 (10^{-5} mol/L) in DASMCs treated with si-negative, si-AC2, or si-AC6 RNA (n=4). **D,** FD6-induced hyaluronan production was attenuated by SB203580 (SB) (2×10^5 mol/L) and H89 (10^6 mol/L) (n=6). **E,** SB203580 (2×10^5 mol/L) did not affect Bnz-cAMP-induced hyaluronan production (n=6). **F,** MKK3 protein expression by Adv.MKK3. MOI indicates multiplicity of infection. **G,** Adv.MKK3 enhanced FD6-induced hyaluronan production (n=6). $^*P<0.05$, $^{**}P<0.01$, $^{***}P<0.001$.

that other AC isoforms might compensate for deficiency of AC6. Alternatively, other EP4 signal pathways in addition to the AC-cAMP pathway may be involved in the patency of EP4KO mice. Further study is required to determine how multiple signaling pathways contribute to yield IT in the DA. We assume that the closure of the DA in AC6KO mice may be delayed after birth because of insufficient IT, which will also be addressed in our future studies.

Interaction of AC2 and AC6 Signaling in Hyaluronan-Mediated IT

AC isoforms have specific patterns of regulation by G proteins, protein kinases and calcium/calmodulin. For example, cAMP production by AC2 is stimulated by several signals including G_s-α and $\beta\gamma$-subunits, and by PKC. In contrast, cAMP production by AC6 is only stimulated by G_s-α and inhibited by G_i-α, PKA, and low concentrations of Ca^{2+}.[4,27] Moreover, different AC isoforms have different effects on cAMP-mediated responses independent of their rate of synthesis of cAMP.[28] To the best of our knowledge, this is the first study to show how the effect of an AC isoform counteracts the effect of another isoform independent of cAMP production. We demonstrated that overexpression of AC2 by itself has little effect on hyaluronan production and appears to have an inhibitory effect on AC6-induced hyaluronan and IT. These data are consistent with the other experiments in which activation of both AC2 and AC6 by FD1 did not induce hyaluronan and IT in DASMCs and DA explants. The response of FD6 to hyaluronan production was much greater than that of FD1, even though FD6 produced less cAMP than FD1 at the same concentrations, suggesting that this process is not simply dependent on the amount of intracellular cAMP.

The next important question is the mechanism how AC2 and AC6 differentially regulate vascular remodeling of the DA. Our results demonstrated that AC6 induced hyaluronan production via the MKK3-p38 MAPK and PKA pathways and that AC2 inhibited the MKK3-p38 pathway, resulting in inhibition of AC6-induced hyaluronan production. PKC, phospholipase C, PI3-kinase, Epac, and other MAPK pathways including ERK and JNK were not involved in AC6-induced hyaluronan production. In addition, we also found that AC2 is primarily localized in the caveolae fraction, whereas AC5/6 localized in the caveolae and the noncaveolae fractions (Online Figure VIII). This differential localization may change the effect of AC2 and AC6 on the downstream signal pathways. Identification of the upstream target linking AC6 and the MKK3-p38 pathways will be addressed in future studies.

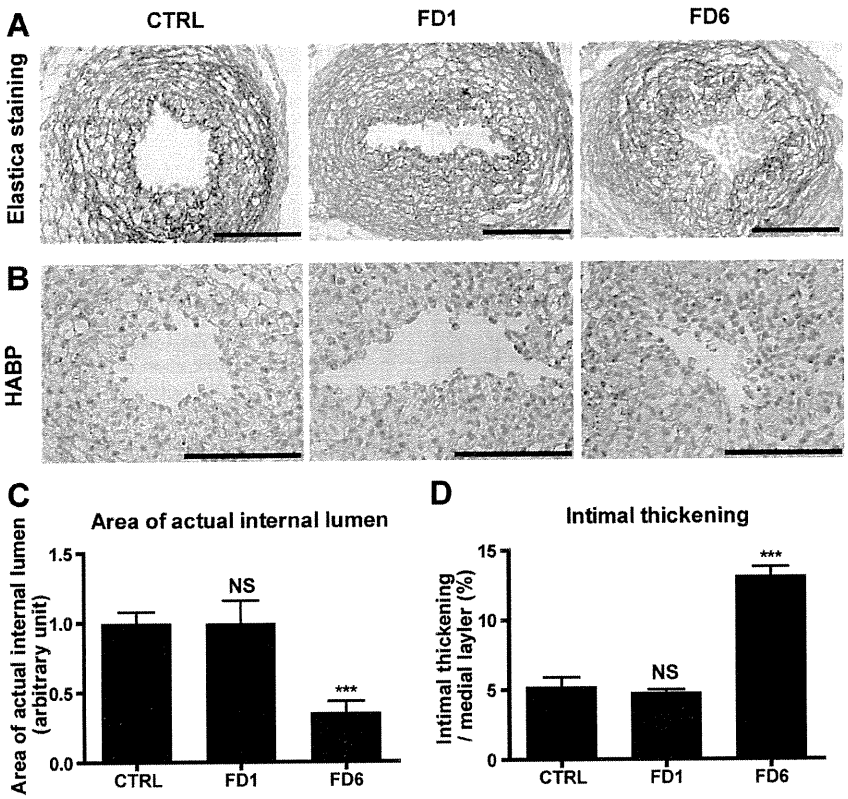

Figure 7. IT in rat DA explants is promoted by FD6. A, Elastica van Gieson staining for DA explants treated with FD1 or FD6. **B,** Strong immunoreaction to hyaluronan in DA explants cultured with FD6. **C,** The area of the internal lumen of the DA treated with FD6 was significantly decreased (n=6 to 7). **D,** The increased IT in the DA treated with FD6 (n=6 to 7). ***$P<0.001$ vs control (CTRL). **Bars:** 100 μm. HABP indicates hyaluronan-binding protein.

Clinical Implications of Using AC Isoform-Selective Modulations

The manipulation of the contractile state of the DA is important for patients with patent DA and complicated congenital heart diseases. All currently available pharmacological therapies rely on synthetic PGE_1 to dilate the DA and prostaglandin H synthase inhibitors to close it. Because these therapies basically change the plasma and/or local concentra-

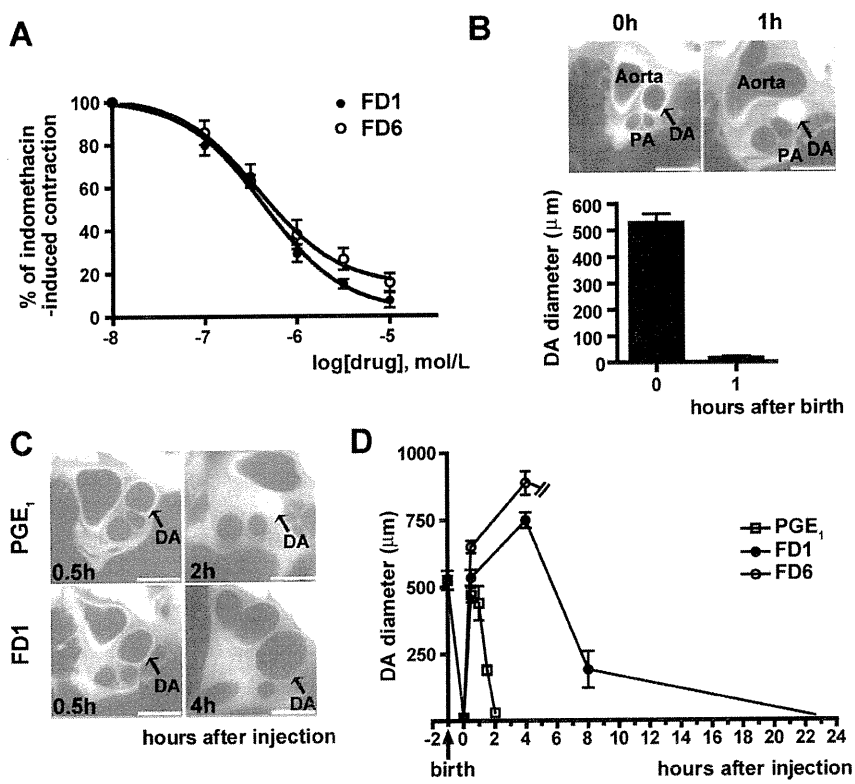

Figure 8. The effects of FD1 and FD6 on vasodilation. A, FD1 and FD6 similarly attenuated indomethacin-induced contraction in DA explants in a dose-dependent manner (n=4 to 10). **B,** The whole-body freezing method revealed that the rat DA opened widely after birth and closed 1 hour after birth **(arrow)** (n=5). **C,** Representative images of rat DAs treated with PGE_1 and FD1 using the whole-body freezing method. **D,** The vasodilating effects of PGE_1, FD1, or FD6 were compared (n=5 to 7). FD1 had a longer action of duration than did PGE_1. All rats injected with FD6 died 4 hours after injection because of apnea. **Bars:** 1 mm. PA indicates pulmonary artery.

tion of PGE, they broadly affect the contractile state and the cellular responses in other types of smooth muscle and tissues, resulting in severe adverse effects on systemic organs. Moreover, PGE_1 has a short duration of action and induces hyaluronan-mediated IT in the DA. In cases of DA-dependent congenital heart diseases, opening of the DA without induction of IT is of particular necessity until the hemodynamics can be improved through surgery. Although differential regulation of vasodilation and IT is preferable for treatment of patients with DA-dependent congenital cardiac malformations, such a treatment is not currently available. Therefore, selective manipulation should be a desirable direction for novel therapeutic strategies. In the present study, we demonstrated that AC isoform-selective activators differentially regulated vascular tone and remodeling in the DA. Our data imply that AC2/6-selective manipulation could be a novel means of achieving DA vasodilation with only minimal effects on the pulmonary arteries and aorta. Moreover, the AC2/6 activator, FD1 has longer pharmacological effects than does PGE_1. Recent studies from other authors have indicated that specific agonists/antagonists for EP4 specifically regulate ductal prostaglandin signals,[29] which could potentially yield a DA-selective vasodilator or vasoconstrictor. However, it should be noted that the EP4 receptor underwent short-term agonist-induced desensitization,[30] which is a common biological phenomenon involving reduction of responsiveness despite continuous agonist induction. Direct activation of AC may overcome the disadvantages of agonist-induced desensitization and FD1 may be beneficial for patients with DA-dependent congenital heart diseases.

In conclusion, we have shown that AC2 and AC6 exert distinct regulation of vascular tone and play an important role in DA remodeling. AC isoform-selective pharmacotherapy using FD1 may serve as a novel therapeutic strategy for patients with DA-dependent congenital heart diseases and as an alternative to currently available PGE therapy.

Acknowledgments

We thank Dr Kazuo Momma and Drs Hideki Taniguchi, Yun-Wen Zheng, and Atsushi Tanaka for assistance with a whole-body freezing method and fluorescence-activated cell sorting analysis, respectively. We thank Dr Koji Otsu for isolation of caveolae fraction.

Sources of Funding

This work was supported by NIH grants 5P01HL066941, HL081741, and HL088426 (to H.K.H.); the Ministry of Health Labor and Welfare of Japan (to Y.I.); the Ministry of Education, Culture, Sports, Science and Technology of Japan (to Y.I. and S.M.); the Yokohama Foundation for Advanced Medical Science (to U.Y., S.M.); the High-Tech Research Center Project for Private Universities: MEXT (to S.M.); Waseda University Grant for Special Research Projects (to S.M.); the Vehicle Racing Commemorative Foundation (to S.M.); Miyata Cardiology Research Promotion Funds (to U.Y. and S.M.); Takeda Science Foundation (to Y.I., U.Y., and S.M.); the Japan Heart Foundation Research Grant (to U.Y.); the Kowa Life Science Foundation (to U.Y.); the Sumitomo Foundation (to U.Y.); the Cosmetology Research Foundation (to Y.I.); Japan Cardiovascular Research Foundation (to S.M.); the Uehara Memorial Foundation (to U.Y.); the Kitsuen Research Foundation (to Y.I.); the Japan Space Forum (to Y.I.); American Heart Association Grant SDG 0835596D (to K.I.); the American Heart Association Western Affiliate (to T.T.); the Department of Veterans Affairs (to H.K.H.); and the Foundation of University of Medicine & Dentistry of New Jersey High-Impact Collaboration Grant (to K.I.).

Disclosures

None.

References

1. Smith GC. The pharmacology of the ductus arteriosus. *Pharmacol Rev.* 1998;50:35–58.
2. Waleh N, Kajino H, Marrache AM, Ginzinger D, Roman C, Seidner SR, Moss TJ, Fouron JC, Vazquez-Tello A, Chemtob S, Clyman RI. Prostaglandin E2–mediated relaxation of the ductus arteriosus: effects of gestational age on g protein-coupled receptor expression, signaling, and vasomotor control. *Circulation.* 2004;110:2326–2332.
3. Yokoyama U, Minamisawa S, Quan H, Ghatak S, Akaike T, Segi-Nishida E, Iwasaki S, Iwamoto M, Misra S, Tamura K, Hori H, Yokota S, Toole BP, Sugimoto Y, Ishikawa Y. Chronic activation of the prostaglandin receptor EP4 promotes hyaluronan-mediated neointimal formation in the ductus arteriosus. *J Clin Invest.* 2006;116:3026–3034.
4. Sunahara RK, Taussig R. Isoforms of mammalian adenylyl cyclase: multiplicities of signaling. *Mol Interv.* 2002;2:168–184.
5. Tang WJ, Gilman AG. Adenylyl cyclases. *Cell.* 1992;70:869–872.
6. Ishikawa Y. Isoform-targeted regulation of cardiac adenylyl cyclase. *J Cardiovasc Pharmacol.* 2003;41(Suppl 1):S1–S4.
7. Bulin C, Albrecht U, Bode JG, Weber AA, Schror K, Levkau B, Fischer JW. Differential effects of vasodilatory prostaglandins on focal adhesions, cytoskeletal architecture, and migration in human aortic smooth muscle cells. *Arterioscler Thromb Vasc Biol.* 2005;25:84–89.
8. Fujino T, Yuhki K, Yamada T, Hara A, Takahata O, Okada Y, Xiao CY, Ma H, Karibe H, Iwashima Y, Fukuzawa J, Hasebe N, Kikuchi K, Narumiya S, Ushikubi F. Effects of the prostanoids on the proliferation or hypertrophy of cultured murine aortic smooth muscle cells. *Br J Pharmacol.* 2002;136:530–539.
9. Indolfi C, Avvedimento EV, Di Lorenzo E, Esposito G, Rapacciuolo A, Giuliano P, Grieco D, Cavuto L, Stingone AM, Ciullo I, Condorelli G, Chiariello M. Activation of cAMP-PKA signaling in vivo inhibits smooth muscle cell proliferation induced by vascular injury. *Nat Med.* 1997;3:775–779.
10. Wang CY, Aronson I, Takuma S, Homma S, Naka Y, Alshafie T, Brovkovych V, Malinski T, Oz MC, Pinsky DJ. cAMP pulse during preservation inhibits the late development of cardiac isograft and allograft vasculopathy. *Circ Res.* 2000;86:982–988.
11. Slomp J, van Munsteren JC, Poelmann RE, de Reeder EG, Bogers AJ, Gittenberger-de Groot AC. Formation of intimal cushions in the ductus arteriosus as a model for vascular intimal thickening. An immunohistochemical study of changes in extracellular matrix components. *Atherosclerosis.* 1992;93:25–39.
12. Pasricha PJ, Hassoun PM, Teufel E, Landman MJ, Fanburg BL. Prostaglandins E1 and E2 stimulate the proliferation of pulmonary artery smooth muscle cells. *Prostaglandins.* 1992;43:5–19.
13. Yau L, Zahradka P. PGE(2) stimulates vascular smooth muscle cell proliferation via the EP2 receptor. *Mol Cell Endocrinol.* 2003;203:77–90.
14. Onda T, Hashimoto Y, Nagai M, Kuramochi H, Saito S, Yamazaki H, Toya Y, Sakai I, Homcy CJ, Nishikawa K, Ishikawa Y. Type-specific regulation of adenylyl cyclase. Selective pharmacological stimulation and inhibition of adenylyl cyclase isoforms. *J Biol Chem.* 2001;276:47785–47793.
15. Iwatsubo K, Minamisawa S, Tsunematsu T, Nakagome M, Toya Y, Tomlinson JE, Umemura S, Scarborough RM, Levy DE, Ishikawa Y. Direct inhibition of type 5 adenylyl cyclase prevents myocardial apoptosis without functional deterioration. *J Biol Chem.* 2004;279:40938–40945.
16. Sutkowski EM, Robbins JD, Tang WJ, Seamon KB. Irreversible inhibition of forskolin interactions with type I adenylyl cyclase by a 6-isothiocyanate derivative of forskolin. *Mol Pharmacol.* 1996;50:299–305.
17. Okumura S, Takagi G, Kawabe J, Yang G, Lee MC, Hong C, Liu J, Vatner DE, Sadoshima J, Vatner SF, Ishikawa Y. Disruption of type 5 adenylyl cyclase gene preserves cardiac function against pressure overload. *Proc Natl Acad Sci U S A.* 2003;100:9986–9990.

18. Tang T, Gao MH, Lai NC, Firth AL, Takahashi T, Guo T, Yuan JX, Roth DM, Hammond HK. Adenylyl cyclase type 6 deletion decreases left ventricular function via impaired calcium handling. *Circulation*. 2008; 117:61–69.
19. Yokoyama U, Minamisawa S, Adachi-Akahane S, Akaike T, Naguro I, Funakoshi K, Iwamoto M, Nakagome M, Uemura N, Hori H, Yokota S, Ishikawa Y. Multiple transcripts of Ca2+ channel alpha1-subunits and a novel spliced variant of the alpha1C-subunit in rat ductus arteriosus. *Am J Physiol Heart Circ Physiol*. 2006;290:H1660–H1670.
20. Gao M, Ping P, Post S, Insel PA, Tang R, Hammond HK. Increased expression of adenylylcyclase type VI proportionately increases beta-adrenergic receptor-stimulated production of cAMP in neonatal rat cardiac myocytes. *Proc Natl Acad Sci U S A*. 1998;95:1038–1043.
21. Wang Y, Huang S, Sah VP, Ross J Jr, Brown JH, Han J, Chien KR. Cardiac muscle cell hypertrophy and apoptosis induced by distinct members of the p38 mitogen-activated protein kinase family. *J Biol Chem*. 1998;273:2161–2168.
22. Yokoyama U, Minamisawa S, Quan H, Akaike T, Suzuki S, Jin M, Jiao Q, Watanabe M, Otsu K, Iwasaki S, Nishimaki S, Sato M, Ishikawa Y. Prostaglandin E2-activated Epac promotes neointimal formation of the rat ductus arteriosus by a process distinct from that of cAMP-dependent protein kinase A. *J Biol Chem*. 2008;283:28702–28709.
23. Akaike T, Jin MH, Yokoyama U, Izumi-Nakaseko H, Jiao Q, Iwasaki S, Iwamoto M, Nishimaki S, Sato M, Yokota S, Kamiya Y, Adachi-Akahane S, Ishikawa Y, Minamisawa S. T-type Ca2+ channels promote oxygenation-induced closure of the rat ductus arteriosus not only by vasoconstriction but also by neointima formation. *J Biol Chem*. 2009;284: 24025–24034.
24. Momma K, Toyoshima K, Takeuchi D, Imamura S, Nakanishi T. In vivo reopening of the neonatal ductus arteriosus by a prostanoid EP4-receptor agonist in the rat. *Prostaglandins Other Lipid Mediat*. 2005;78:117–128.
25. Yokoyama U, Patel HH, Lai NC, Aroonsakool N, Roth DM, Insel PA. The cyclic AMP effector Epac integrates pro- and anti-fibrotic signals. *Proc Natl Acad Sci U S A*. 2008;105:6386–6391.
26. Rabinovitch M, Beharry S, Bothwell T, Jackowski G. Qualitative and quantitative differences in protein synthesis comparing fetal lamb ductus arteriosus endothelium and smooth muscle with cells from adjacent vascular sites. *Dev Biol*. 1988;130:250–258.
27. Wong ST, Baker LP, Trinh K, Hetman M, Suzuki LA, Storm DR, Bornfeldt KE. Adenylyl cyclase 3 mediates prostaglandin E_2-induced growth inhibition in arterial smooth muscle cells. *J Biol Chem*. 2001;276:34206–34212.
28. Gros R, Ding Q, Chorazyczewski J, Pickering JG, Limbird LE, Feldman RD. Adenylyl cyclase isoform-selective regulation of vascular smooth muscle proliferation and cytoskeletal reorganization. *Circ Res*. 2006;99: 845–852.
29. Kajino H, Taniguchi T, Fujieda K, Ushikubi F, Muramatsu I. An EP4 receptor agonist prevents indomethacin-induced closure of rat ductus arteriosus in vivo. *Pediatr Res*. 2004;56:586–590.
30. Nishigaki N, Negishi M, Ichikawa A. Two Gs-coupled prostaglandin E receptor subtypes, EP2 and EP4, differ in desensitization and sensitivity to the metabolic inactivation of the agonist. *Mol Pharmacol*. 1996; 50:1031–1037.

Novelty and Significance

What Is Known?

- Prostaglandin (PG)E-adenylyl cyclase (AC)-cAMP signaling opens the ductus arteriosus (DA) by vasodilation and closes it by hyaluronan-mediated intimal thickening.
- Differential regulation of vasodilation and remodeling of the DA is required for patients with DA-dependent congenital heart diseases after birth.

What New Information Does This Article Contribute?

- AC type 6 (AC6) is involved in vasodilation and hyaluronan-mediated intimal thickening.
- AC type 2 (AC2) inhibits AC6-induced intimal thickening.
- Stimulation of both AC2 and AC6 by the new forskolin derivative FD1 induced long-lasting vasodilation without intimal thickening in the DA.

PGE plays 2 opposing roles in the DA: it induces opening of the DA by vasodilation, and closure by hyaluronan-mediated intimal thickening. Dilation of the DA, but not intimal thickening, is necessary in patients with DA-dependent congenital heart diseases after birth. However, the currently available PGE therapy is not able to differentially regulate vasodilation and intimal thickening in the DA. Our results suggest that AC6 plays a primary role in hyaluronan-mediated vascular remodeling and vasodilation in the DA and that AC2 has an inhibitory effect on AC6-mediated vascular remodeling. We found that stimulation of both AC2 and AC6 by the forskolin derivative FD1 induced long-lasting vasodilation without intimal thickening in the DA. For the first time, we demonstrated that AC2 and AC6 exert distinct regulation of vascular tone and remodeling. In particular, our identification of the interaction of two signaling pathways of AC isoforms in vascular remodeling is novel. AC isoform-selective pharmacotherapy using FD1 may yield a new therapeutic strategy for patients with DA-dependent congenital heart diseases who require DA opening, but not DA closure, through hyaluronan-mediated neointimal thickening. This may become an alternative to the currently available PGE therapy.

THE JOURNAL OF BIOLOGICAL CHEMISTRY VOL. 285, NO. 31, pp. 24248–24259, July 30, 2010

Differential Roles of Epac in Regulating Cell Death in Neuronal and Myocardial Cells*[S]

Received for publication, December 21, 2009, and in revised form, May 13, 2010 Published, JBC Papers in Press, June 1, 2010, DOI 10.1074/jbc.M109.094581

Sayaka Suzuki[‡], Utako Yokoyama[‡1], Takaya Abe[§], Hiroshi Kiyonari[§], Naoya Yamashita[¶], Yuko Kato[‡], Reiko Kurotani[‡], Motohiko Sato[‡], Satoshi Okumura[‡], and Yoshihiro Ishikawa[‡‖]

From the [‡]Cardiovascular Research Institute and [¶]Department of Molecular Pharmacology and Neurobiology, Yokohama City University Graduate School of Medicine, Yokohama 236-0004, Japan, the [§]Laboratory for Animal Resources and Genetic Engineering, RIKEN Center for Developmental Biology, Kobe 650-0047, Japan, and the [‖]Cardiovascular Research Institute, Departments of Cell Biology and Molecular Medicine, and the Department of Medicine, New Jersey Medical School-University of Medicine and Dentistry of New Jersey, Newark, New Jersey 07103

Cell survival and death play critical roles in tissues composed of post-mitotic cells. Cyclic AMP (cAMP) has been known to exert a distinct effect on cell susceptibility to apoptosis, protecting neuronal cells and deteriorating myocardial cells. These effects are primarily studied using protein kinase A activation. In this study we show the differential roles of Epac, an exchange protein activated by cAMP and a new effector molecule of cAMP signaling, in regulating apoptosis in these cell types. Both stimulation of Epac by 8-*p*-methoxyphenylthon-2′-*O*-methyl-cAMP and overexpression of Epac significantly increased DNA fragmentation and TUNEL (terminal deoxynucleotidyltransferase-mediated biotin nick end-labeling)-positive cell counts in mouse cortical neurons but not in cardiac myocytes. In contrast, stimulation of protein kinase A increased apoptosis in cardiac myocytes but not in neuronal cells. In cortical neurons the expression of the Bcl-2 interacting member protein (Bim) was increased by stimulation of Epac at the transcriptional level and was decreased in mice with genetic disruption of Epac1. Epac-induced neuronal apoptosis was attenuated by the silencing of Bim. Furthermore, Epac1 disruption *in vivo* abolished the 3-nitropropionic acid-induced neuronal apoptosis that occurs in wild-type mice. These results suggest that Epac induces neuron-specific apoptosis through increasing Bim expression. Because the disruption of Epac exerted a protective effect on neuronal apoptosis *in vivo*, the inhibition of Epac may be a consideration in designing a therapeutic strategy for the treatment of neurodegenerative diseases.

Induction of apoptosis in post-mitotic cells, such as neurons and cardiac myocytes, has been thought to be responsible for such irreversible disorders as Alzheimer and Huntington diseases as well as stroke and heart failure (1). The effect on cell death of cyclic AMP (cAMP), a major second messenger, has been extensively studied. In neuronal cells it is well known that activation of cAMP signals reduces the rate of neuronal cell death under a variety of stresses (*i.e.* β-amyloid protein, sialoglycopeptide, low potassium-induced neurotoxicity) (2–4), although there have been several reports that dopamine or prostanoid receptor-mediated cAMP production induces neurotoxicity (5, 6). β-Adrenergic receptor signaling, on the other hand, promotes apoptosis in cardiac myocytes, resulting in heart failure (7, 8). Therefore, the model proposing that cAMP signaling plays a protective role in neuronal cells but a deteriorative role in myocardial cells is well accepted.

Most studies that have demonstrated the effect of cAMP signaling on apoptosis have focused primarily on protein kinase A (PKA),[2] a classic target molecule of cAMP. Recent studies involving cAMP signaling have focused instead on Epac, an exchange protein activated by cAMP that has been identified as a new target of cAMP, independent of PKA (9). Epac has been found to regulate a variety of cellular processes, including cell proliferation, migration, secretion, and differentiation (10). It has been demonstrated that Epac either alone or with PKA plays a protective role in immune cells against apoptosis (11, 12). In post-mitotic cells such as neurons and cardiac myocytes, however, the role of Epac in apoptosis has not been reported.

To date two isoforms of Epac have been identified, Epac1 and Epac2 (9); they differ in that Epac2 contains a second binding site for cAMP. It has recently been reported that there is an up-regulation of Epac1 mRNA in Alzheimer disease (13) and an up-regulation of Epac1 protein expression in rats with inflamed neurons (14), implicating that cAMP signaling may not always play a protective role in neurons. The change in the Epac1 expression pattern has also been demonstrated in other cell

* This work was supported by a grant-in-aid for Scientific Research (KAKENHI) (to U. Y. and S. S.) and by grants from the Ministry of Health, Labor, and Welfare (to Y. I.), the Ministry of Education, Culture, Sports, Science, and Technology of Japan (to Y. I.), the Yokohama Foundation for Advanced Medical Science (to U. Y.), the Kanae Foundation for the Promotion for Medical Science (to U. Y.), the Miyata Cardiology Research Promotion Funds (to U. Y.), the Takeda Science Foundation (to U. Y.), the Sumitomo Foundation (to U. Y.), the Japan Heart Foundation Research Grant (to U. Y.), the Kowa Life Science Foundation (to U. Y.), the Cosmetology Research Foundation (to Y. I.), the Uehara Memorial Foundation (to U. Y.), the Kitsuen Research Foundation (to Y. I.), and the Japan Space Forum (to Y. I.).

[S] The on-line version of this article (available at http://www.jbc.org) contains supplemental Methods and Figs. 1–7.

[1] To whom correspondence should be addressed: Cardiovascular Research Institute, Yokohama City University Graduate School of Medicine, 3-9 Fukuura, Kanazawa-ku, Yokohama 236-0004, Japan. Tel.: 81-45-787-2575; Fax: 81-45-788-1470; E-mail: utako@yokohama-cu.ac.jp.

[2] The abbreviations used are: PKA, protein kinase A; Bim, Bcl-2 interacting member protein; pMe-cAMP, 8-*p*-methoxyphenylthon-2′-*O*-methyl-cAMP; Bnz-cAMP, N^6-benzoyladenosine-cAMP; RT, reverse transcription; TUNEL, terminal deoxynucleotidyltransferase-mediated biotin nick end-labeling; 3-NP, 3-propionic acid; siRNA, small interfering RNA; DAPI, 4′,6-diamidino-2-phenylindole; JNK, c-Jun N-terminal kinase; MAPK, mitogen-activated protein kinase; KO, knock-out.

types (*i.e.* heart, vasculature, kidney, and lung) (15–18). The stoichiometry of Epac, especially of Epac1, and that of PKA might be changed in several diseases, including neuronal and cardiac disorders; this could lead to the various effects of cAMP signaling on cell death.

Through experiments using Epac- or PKA-selective cAMP analogs and overexpression of Epac1 and the PKA catalytic subunit and Epac1-deficient mice, the present study demonstrates that cAMP signaling no longer increases neuronal cell viability when Epac is selectively activated: instead, cAMP signaling induces apoptosis through increasing Bcl-2 interacting member protein (Bim) expression. Our findings also suggest that the selective inhibition of Epac signaling may become a therapeutic strategy in the treatment of neurodegenerative diseases.

EXPERIMENTAL PROCEDURES

Antibodies and Reagents—8-*p*-Methoxyphenylthon-2′-*O*-methyl-cAMP (pMe-cAMP) and N^6-benzoyladenosine-cAMP (Bnz-cAMP) were purchased from BioLog Life Science Institute (Bremen, Germany) and Sigma, respectively. Antibodies to Epac1, Epac2, and a PKA α catalytic subunit were obtained from Santa Cruz Biotechnology (Santa Cruz, CA). An antibody to Bim was purchased from Stressgen Biotechnologies (Victoria, BC, Canada). Antibodies to Bim and cleaved caspase 3 were purchased from Cell Signaling Technology (Danvers, MA). An antibody to Bcl-2 was purchased from BD Biosciences.

Generation of Epac1 Knock-out Mice—Epac1 knock-out mice (Epac1 KO; accession number CDB0542K (LARGE (Laboratory for Animal Resources and Genetic Engineering)) were generated by means of homologous recombination (19). Briefly, the targeting vector was constructed by inserting loxP/PGK-Neo-pA/loxP (LARGE) into exon 1 and exon 2 of the genomic Epac1 locus (see Fig. 7*A*). The targeting vector was introduced into TT2 embryonic stem cells, and homologous recombinant clones were first identified by PCR, then confirmed by Southern blot analysis (see Fig. 7*B*). The targeted embryonic stem cell clones were injected into CD-1 8-cell stage embryos, and the resultant male chimeras were mated with C57BL/6 females to establish germ line transmission. All experiments were performed on C57BL/6 and CBA mixed-background 3–5-month-old male homozygous Epac1 KO and wild type (WT) littermates from F1 heterozygote crosses. Mice were genotyped by PCR using a mixture of three primers (F1, TGA GAA GAG CCC CAT CGT TGT G; B1, GCC TGG CAC ATG GAA GTG AT; NeoF1, TGA ATG GAA GGA TTG GAG CTA CG) as indicated in Fig. 7*A*. The PCR conditions consisted of 95 °C for 5 min, 35 cycles of 95 °C for 30 s each, 60 °C for 30 s, and 72 °C for 30 s followed by 72 °C for 7 min (Fig. 7*C*).

All experiments were performed on 3–5-month-old homozygous Epac1 KO mice and WT littermates. This study was approved by the Animal Care and Use Committee at Yokohama City University School of Medicine.

Primary Culture of Fetal Mouse Cortical Neurons—Primary cortical neurons were isolated from the cortices of embryonic day 15–17 C57BL/6 or Epac1 KO mice, as previously described (20) with some modifications. Briefly, the cortex was incubated with 0.3% trypsin (Invitrogen) by titration; then cells were plated onto a 12-mm glass coverslip precoated with 6 mg/ml poly-L-lysine (Wako Pure Chemical Industries, Osaka, Japan) at a density of 1×10^5 cells/glass. The cells were incubated at 37 °C with 5% CO_2, 95% atmospheric air in a neurobasal medium containing 1× GlutaMAX-1, B-27 supplement (Invitrogen), 100 μg/ml penicillin, and 100 μg/ml streptomycin. Cells were used in experiments 4–7 days later.

Primary Culture of Neonatal Mouse Cardiac Myocytes—Cardiac myocytes were isolated from the hearts of 1-day-old mice as previously described (21) with some modifications. Briefly, myocytes were chopped into small pieces and digested with 0.1% collagenase type II and 0.04% pancreatin 3 times at 7-min intervals. To remove the non-myocyte fraction, the cells were plated onto culture dishes in minimum essential medium (Invitrogen) with 10% fetal bovine serum containing 100 μg/ml penicillin and 100 μg/ml streptomycin for 45 min, after which the non-attached myocyte-rich fraction was plated onto a 12-mm glass coverslip precoated with 20 mg/ml laminin (Sigma) at a density of 1×10^5 cells/glass in the same medium. Twenty-four hours after plating, the culture medium was changed to minimum essential medium with an insulin-transferrin-selenium-A supplement (ITS-A, Invitrogen) containing 100 μg/ml penicillin and 100 μg/ml streptomycin. The cells were maintained in a humidified 5% CO_2, 95% atmospheric air incubator at 37 °C.

Primary Culture of Mouse Renal Epithelial Cells—Primary culture of mouse renal epithelial cells was performed as previously described (22).

Quantitative Reverse Transcription (RT)-PCR—Total RNA was extracted from cortical neurons using TRIzol (Invitrogen) according to the manufacturer's instructions. Both the generation of cDNA and the RT-PCR analysis were performed as previously described (17, 23). Real-time PCR was executed using a MyiQ Single-Color Real-Time PCR Detection System (Bio-Rad) and an SYBR Green kit (Takara Bio, Shiga, Japan). Primers for amplification were designed based on Bim (5′-CCCGGAGAT-ACGGATTGCAC-3′ and 5′- GCCTCGCGGTAATCATTTGC-3′) and 18 S ribosomal RNA. The forward and reverse primer set was designed between multiple exons. Abundance of mRNA was determined relative to that of 18 S ribosomal RNA.

Northern Blotting—Partial fragments of mouse Epac1 and Epac2 cDNA clones were obtained by PCR. A mouse glyceraldehyde-3-phosphate dehydrogenase probe was used as an internal control. Northern blotting was performed as previously described (24).

Western Blot Analysis—Western blot analysis of cortical neurons and cardiac myocytes was performed as previously described (25) with some modifications. Briefly, cells in 35-mm plastic dishes were lysed and collected with a lysis buffer (25 mM Tris-HCl (pH 8.0), 10 mM EGTA, 10 mM EDTA, 10 mM $Na_4P_2O_7$, 100 mM NaF, 10 mM Na_3VO_4, 20 μg/ml 1-chloro-3-tosylamido-7-amino-2-heptanone or N^{α}-*p*-tosyl-L-lysine chloromethyl ketone, 10 μg/ml leupeptin, 1 mM phenylmethylsulfonyl fluoride, 50 units of erythrina trypsin inhibitor, 2 μg/ml aprotinin, and 1% Nonidet P-40). After protein concentrations were determined using the RC DC protein assay kit (Bio-Rad), SDS-PAGE and Western blotting were performed followed by densitometric analysis using LAS3000 and Science Lab Multi Gauge Version 3.0 software (Fujifilm, Tokyo, Japan).

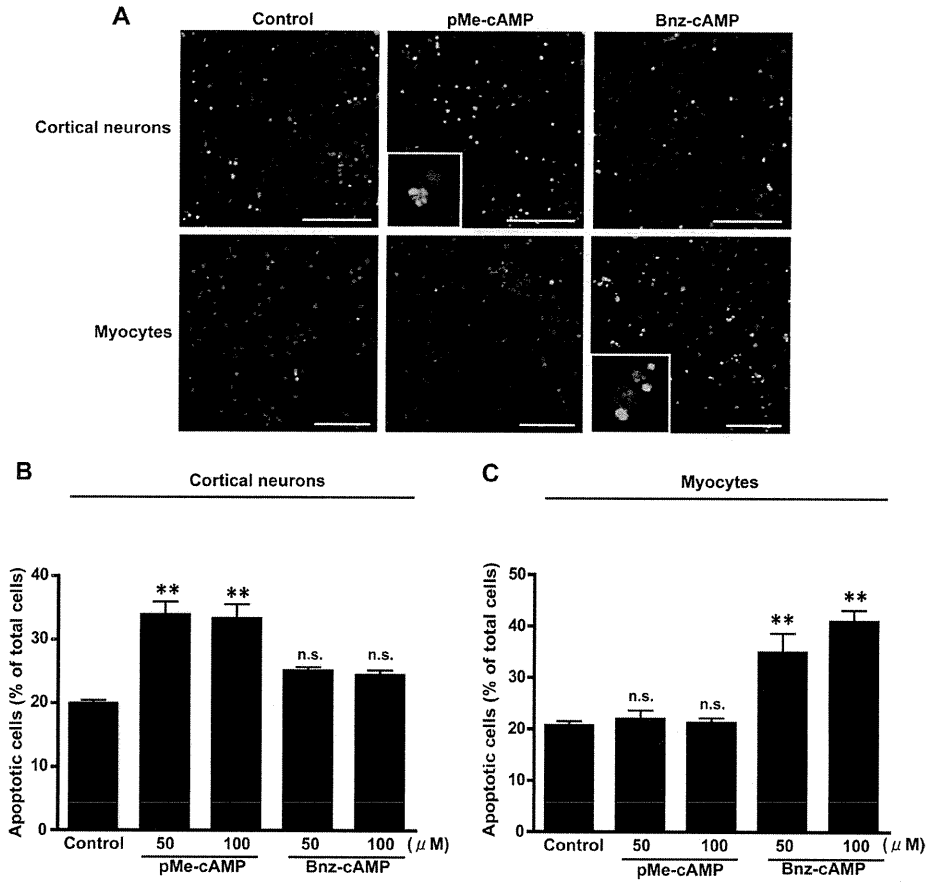

FIGURE 1. **Effects of activation of Epac and PKA on apoptosis in cortical neurons and cardiac myocytes.** *A*, apoptotic cells (*green*) in cortical neurons and myocytes were examined by means of TUNEL staining 48 h after treatment with pMe-cAMP (50 μM) or Bnz-cAMP (50 μM). Nuclei were stained with DAPI (*blue*). *Scale bar*, 100 μm. The *inset* is magnified five additional times. *B* and *C*, quantification of TUNEL-positive cells by counting nuclei in cortical neurons and cardiac myocytes is shown. The results are presented as percentages of the total cell number. $n = 6$ from 3 independent experiments. **, $p < 0.01$ *versus* control. *n.s.*, not significant.

Immunoprecipitation—Lysates from cells treated with pMe-cAMP or Bnz-cAMP for 24 h were incubated with 2 μg of anti-Bcl-2 or anti-Bim antibody overnight. Immune complexes were captured with protein G-Sepharose 4 Fast Flow (GE Healthcare). Beads were washed 3 times in the lysis buffer and boiled in an SDS sample buffer. Samples were subjected to SDS-PAGE and blotted onto a polyvinylidene difluoride membrane (Immobilon-P; Millipore, Billerica, MA).

Adenovirus Construction—For construction of adenoviral vectors, full-length cDNA-encoding human Epac1, Epac2, and PKA α catalytic subunits were cloned into an adenoviral vector using an AdenoX adenovirus construction kit (Clontech, Mountain View, CA) (17). Human Epac1 and Epac2 cDNAs were kindly provided by Dr. J. L. Bos of University Medical Center, Utrecht, The Netherlands. Adenovirus-mediated transfection was performed using LacZ control. The cells were infected with adenoviruses at the indicated multiplicities of infection and used for their corresponding assays 24 h later.

Transfection of siRNA in Cortical Neurons—Silencing of Bim was carried out using Accell SMARTpool siRNAs (Dharmacon Inc., Lafayette, CO), each of which contains four siRNAs designed for use with the Bim gene (5′-CUGGCUUCCUUUACGUUUU-3′, 5′-CUAUGAAUUGUAGAAGUAU-3′, 5′-CGCUUAUUUAA-AUGUCUUA-3′, and 5′-UCAUAA-UUAAGGAUUUGUA-3′) according to the manufacturer's instructions. Briefly, 48 h after plating, cortical neurons were transfected with 1 μM siRNA and subsequently cultured in a neurobasal medium. The efficiency of the knockdown of the Bim protein was evaluated 72 h after transfection by Western blot analysis. Scrambled siRNAs for Bim-targeted siRNA (Dharmacon Inc.) were used as a negative control.

Terminal Deoxynucleotidyltransferase-mediated Biotin Nick End-labeling (TUNEL) Assay—*In situ* labeling of fragmented DNA in cultured cortical neurons and cardiac myocytes was performed using the DeadEnd™ fluorometric TUNEL system (Promega, Madison, WI) according to the manufacturer's instructions. Cells were incubated with the presence or absence of pMe-cAMP or Bnz-cAMP for 48 h, fixed with 4% paraformaldehyde for 25 min, and then incubated with 0.2% Triton X-100 for 5 min. The cells were equilibrated with a buffer consisting of 200 mM potassium cacodylate (pH 6.6), 25 mM Tris-HCl (pH 8.0), 0.2 mM dithiothreitol, 0.25 mg/ml bovine serum albumin, and 2.5 mM cobalt chloride at room temperature for 10 min followed by 60 min of incubation with a terminal deoxynucleotidyltransferase reaction buffer containing 100 μM dATP, 5 μM fluorescein-12-dUTP, 10 mM Tris-HCl (pH 7.6), 1 mM EDTA, and 40 μM terminal deoxynucleotidyltransferase enzyme at 37 °C. DNAs were stained with DAPI (4′, 6-diamidino-2 phenylindole). The percentage of the total cells that were TUNEL-positive was determined in a blinded manner. Approximately 2000–3000 cells in 10 randomly selected fields from each sample were counted. For detection of apoptosis in brain tissues from WT or Epac1 KO mice, deparaffinized tissue sections were treated with 20 μg/ml proteinase K and 50 mM EDTA in 100 mM Tris-HCl (pH 8.0). The sections were fixed with 4% paraformaldehyde for 15 min at room temperature and then subjected to the equilibration step in the procedures described above.

Analysis of DNA Fragmentation by Enzyme-linked Immunosorbent Assay—Histone-associated DNA fragments were quantified using the Cell Death Detection enzyme-linked immunosorbent assay kit (Roche Diagnostics) according to the manufacturer's instructions. After cortical neurons and cardiac myocytes were incubated in the presence or absence of pMe-cAMP or Bnz-cAMP for 48 h, they were gently washed with phosphate-buffered saline and incubated with a lysis buffer

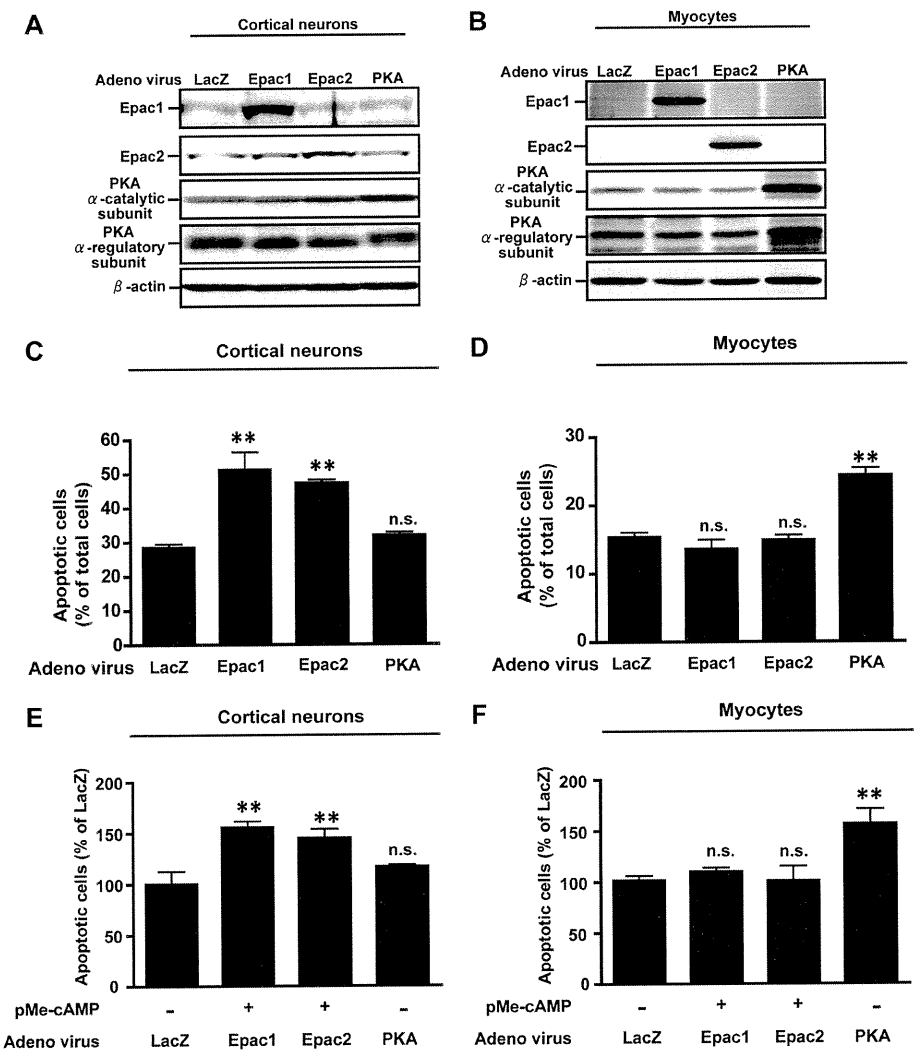

FIGURE 2. **Effects of overexpression of Epac and PKA on apoptosis in cortical neurons and cardiac myocytes.** *A*, shown are the representative immunoblots of cortical neurons or myocytes transfected with Epac1, Epac2, PKA α catalytic subunit, PKA regulatory subunit, and LacZ for 12 h (multiplicity of infection = 2). β-Actin served as an internal control. *C–F*, apoptosis was evaluated by means of TUNEL staining (*C* and *D*) and cell death detection enzyme-linked immunosorbent assay (*E* and *F*) 48 h after incubation with indicated adenovirus and an Epac-selective cAMP analog in cortical neurons and cardiac myocytes. The results are presented as percentages of the total cell number. $n = 4-8$ from 2 independent experiments. **, $p < 0.01$, *versus* LacZ control. *n.s.*, not significant.

(phosphate-buffered saline containing 10 mM EDTA (pH 7.2) and 0.1% Triton-X) for 1 h at 37 °C followed by vigorous shaking for 30 s. The cell lysates containing cytoplasmic histone-associated DNA fragments were applied to a streptavidin-coated microtiter plate. Subsequently, a mixture of biotin-labeled anti-histone antibody and peroxidase-conjugated anti-DNA antibody was added, and the resulting mixture was incubated with moderate shaking for 2 h. After unbound antibodies were removed by washing, the amount of nucleosomes was quantified based on the peroxidase retained in the immune complex. The activity of the peroxidase was determined photometrically using 2,2-azino-di-[3-ethylbenzthiazoline-sulfonate] as a substrate. The values from triplicate absorbance (at 405 nm) measurements were then averaged.

Mitochondrial Membrane Potential Analysis—Mitochondrial membrane potential of cortical neurons was quantified using a Mitocapture™ Mitochondrial Apoptosis Detection kit (BioVision Inc., Mountain View, CA) according to the manufacturer's instructions. Cortical neurons were incubated on a 12-mm glass coverslip in the presence or absence of pMe-cAMP or Bnz-cAMP for 48 h, then stained with Mitocapture reagent and incubated in DAPI to allow the visualization of all nuclei. The images were obtained using an inverted microscope (TE2000-E, Nikon, Japan). The red emission of the dye detected at 543 nm is due to a potential-dependent aggregation in the mitochondria reflecting normal membrane potential. Green fluorescence detected at 488 nm reflects the monomeric form of Mitocapture™, appearing in the cytosol after mitochondrial membrane depolarization. The percentage of the total cells representing apoptotic cells was determined in a blinded manner by counting ~1000–3000 cells in 10 randomly selected fields from each sample.

Rap1 Activation Assay—Rap1 activity was measured using the EZ-Detect RAP1 activation kit (Pierce) according to the manufacturer's instructions. Primary renal epithelial cells from WT and Epac1 KO mice were lysed 15 min after stimulation with pMe-cAMP (50 μM). Cell lysates were incubated with the Rap binding domain RalGDS-RBD fused to a glutathione *S*-transferase disk. After cells were washed several times, bound GTP-Rap1 was removed from the disk through boiling in an SDS sample buffer and analyzed by Western blotting using an anti-Rap1 antibody.

In Vivo Experiment and Tissue Preparation—3-Propionic acid (3-NP, Sigma) was prepared and administered as previously described (26). 3-NP was dissolved in saline, and the resulting solution was adjusted to pH 7.3–7.4 with 5 N NaOH. 3-NP (140 mg/kg/day) was the injected intraperitoneally into the animals once per day for 2 days. Twenty-four hours after the second injection, the mice were anesthetized with pentobarbital and transcardially injected with 10% paraformaldehyde/phosphate-buffered saline (pH 7.4). Brains were fixed in the same fixative solution overnight, immersed in 70% ethanol for 24 h, then embedded in paraffin. Sections 4 μm in thickness were subjected to TUNEL staining.

Statistical Analysis—All data are reported as the mean ± S.E. Comparisons between two groups were analyzed using Student's *t* test. For multiple groups, one-way analysis of variance

was used with a Bonferroni post-hoc test. $p < 0.05$ was considered to indicate significance.

RESULTS

Differential Effects of Epac on Apoptosis in Mouse Cortical Neurons and Myocytes—We first investigated whether the stimulation of Epac has similar effects on apoptosis in various kinds of post-mitotic cells using a primary culture of mouse cortical neurons and cardiac myocytes. Apoptosis was detected by means of TUNEL staining 48 h after treatment with pMe-cAMP or Bnz-cAMP, the Epac- and PKA-selective cAMP analogs, respectively (27). We observed strong TUNEL labeling of apoptotic bodies in cortical neurons treated with pMe-cAMP (Fig. 1*A*, *upper panels*, *inset*). In contrast, pMe-cAMP did not induce apoptosis in cardiac myocytes (Fig. 1*A*, *lower panels*). The number of TUNEL-positive cells was quantified, showing that stimulation of Epac significantly increased apoptosis in cortical neurons but not in cardiac myocytes (Fig. 1, *B* and *C*). Because a high Bax/Bcl-2 ratio is associated with greater vulnerability to apoptotic activation (28, 29), we quantified the protein expression of Bax/Bcl-2 to confirm our findings. Activation of Epac by pMe-cAMP increased the Bax/Bcl-2 ratio in cortical neurons but not in cardiac myocytes (supplemental Fig. 1, *A–D*).

It is already known that activation of cAMP/PKA signaling plays a protective role in neuronal cells but a deteriorative role in myocardial cells (30, 31). In accordance with previous reports, the PKA-selective cAMP analog Bnz-cAMP induced apoptosis in cardiac myocytes but not in cortical neurons, even at 100 μM (Fig. 1, *A–C*). These results suggest that the activation of Epac has different effects on apoptosis in neuronal cells and cardiac myocytes.

Effects of Overexpression of Epac on Apoptosis in Cortical Neurons and Cardiac Myocytes—To confirm that Epac was involved in neuronal cell death, we performed adenovirus-mediated gene transfer of Epac1 and Epac2 (as both isoforms of Epac (9) are known to be activated by pMe-cAMP), a PKA α catalytic subunit, or a LacZ control. Overexpression of Epac1, Epac2, PKA α catalytic subunit proteins, or PKA α regulatory subunit proteins in cortical neurons and cardiac myocytes 12 h after infection with each adenovirus is shown in Fig. 2, *A* and *B*. Endogenous protein expression of Epac1, Epac2, and PKA subunits was not significantly affected by any of the adenoviruses. We also confirmed that overexpression of PKA α catalytic subunit significantly increased PKA activity in cortical neurons (supplemental Fig. 2). Overexpression of Epac1 or Epac2, unlike LacZ, significantly increased the incidence of TUNEL-positive apoptotic cells in cortical neurons but not in cardiac myocytes (Fig. 2, *C* and *D*). In contrast, overexpression of PKA increased the number of TUNEL-positive cells in cardiac myocytes but not in cortical neurons. An enzyme-linked immunosorbent assay yielded results similar to those of TUNEL staining (Fig. 2, *E* and *F*), indicating that overexpression of Epac1 or Epac2 increased DNA fragmentation in cortical neurons but not in cardiac myocytes. Importantly, these results are different from those obtained through PKA overexpression, suggesting that, at least in part, Epac promotes neuronal, but not myocardial, apoptosis.

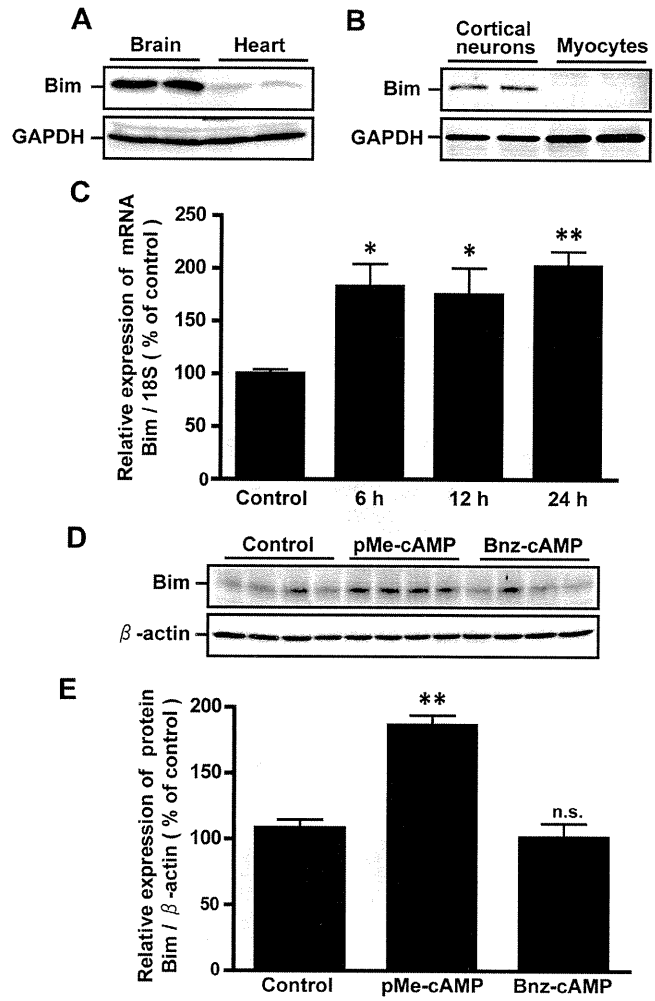

FIGURE 3. **Activation of Epac increased the expression of Bim mRNA and protein in cortical neurons.** *A* and *B*, shown is expression of endogenous Bim protein in brain and heart tissues (*A*) and cultured cortical cells and cardiac myocytes (*B*). *C*, the expression of Bim mRNA in cortical neurons was quantified using real-time RT-PCR. The data are normalized to 18 S ribosomal RNA. *D*, shown are representative immunoblots of Bim 24 h after the addition of pMe-cAMP (50 μM) or Bnz-cAMP (50 μM) in cortical neurons. β-Actin served as an internal control. *E*, shown is quantification of cAMP analog-induced Bim expression from three independent experiments. The results are presented as percentages of the amount of Bim expressed in the control experiment. $n = 6–8$, **, $p < 0.01$ *versus* control. *GAPDH*, glyceraldehyde-3-phosphate dehydrogenase.

Epac Activation Increases Bim Expression—The Bcl-2 interacting member (Bim) is a sensor of apoptotic stress located upstream of the Bcl-2 family. Bim regulates Bcl-2 in the mitochondrial membrane, resulting in apoptosis (32, 33). Bim protein was highly expressed in brain tissue and cortical neurons (Fig. 3, *A* and *B*) but was expressed either slightly or not at all in heart tissue and cardiac myocytes, as previously described (34, 35). A previous paper suggested the involvement of cAMP/PKA signaling in regulating Bim expression in lymphoid cells (55). We, therefore, examined the change in the expression levels of Bim mRNA and protein in cortical neurons using pMe-cAMP. We found that pMe-cAMP increased expression of Bim mRNA and protein in a time-dependent manner (Fig. 3*C* and see Fig. 5, *C* and *F*). Furthermore, pMe-cAMP, but not Bnz-cAMP, signif-

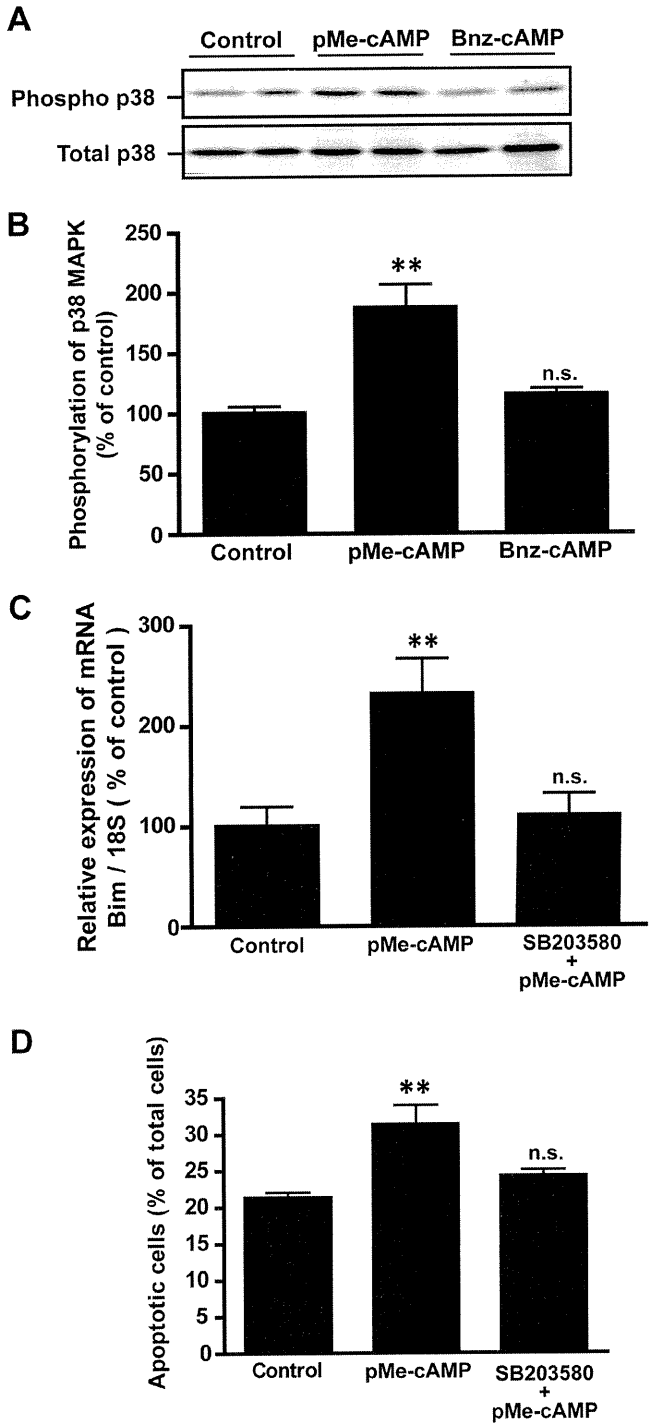

FIGURE 4. **Effect of p38 MAPK on Epac-induced Bim expression and apoptosis in cortical neurons.** *A* and *B*, shown are representative images and quantification of phosphorylation/total p38 protein in mouse cortical neurons treated with pMe-cAMP (50 μM) or Bnz-cAMP (50 μM) for 24 h. The results are presented as percentages of the amount of phosphorylation observed in the control experiment. $n = 6$ from 3 independent experiments. **, $p < 0.01$ *versus* control. *C*, the expression of Bim mRNA 24 h after the addition of pMe-cAMP (50 μM) or SB203580 (10 μM) plus pMe-cAMP (50 μM) in cortical neurons was quantified using real-time RT-PCR. The data are normalized to 18 S ribosomal RNA. $n = 6-8$; **, $p < 0.01$ *versus* control. *D*, apoptotic cells in cortical neurons and myocytes were examined by means of TUNEL staining 48 h after treatment with pMe-cAMP (50 μM) or SB203580 (10 μM) plus pMe-cAMP (50 μM). TUNEL-positive cells were quantified by counting nuclei in cortical neurons. The results are presented as percentages of the total cell number. $n = 4-6$; **, $p < 0.01$ *versus* control. *n.s.*, not significant.

icantly increased Bim protein in cortical neurons 24 h after treatment (Fig. 3,*D* and *E*). These results suggest that the stimulation of Epac increases Bim expression by enhancing transcription in cortical neurons, although the stimulation of PKA does not.

Inhibition of p38 MAPK Attenuates Epac-induced Bim Expression and Apoptosis—Three signal pathways have been implicated in regulating Bim protein expression: the JNK/c-Jun, cell cycle (Cdk4/E2F/Myb), and p38MAPK/FoxO pathways (36, 37). We next sought to determine which of these pathways plays the most important role. We found that an Epac-selective cAMP analog increased phosphorylation of p38 MAPK in cortical neurons, although a PKA-selective cAMP analog did not (Fig. 4, *A* and *B*). In contrast, there was no significant difference between Epac and PKA stimulation in terms of their effects on the phosphorylation of p44/42 MAPK, JNK1, or JNK2/3 (data not shown). Furthermore, SB203580, a p38 MAPK inhibitor, attenuated Epac-induced Bim expression and apoptosis (Fig. 4, *C* and *D*). These results suggest that Epac-induced neuronal apoptosis is mediated by the elevation of Bim expression via p38 MAPK.

Epac Activation Increases Interaction of Bim with Bcl-2—Bim is thought to exert its pro-apoptotic activity by binding to Bcl-2, thereby blocking the anti-apoptotic function of Bcl-2 (38). After demonstrating that stimulation of Epac increased Bim expression, we needed to confirm that the binding of Bim to Bcl-2 was likewise increased. We conducted pulldown assays using anti-Bcl-2 and anti-Bim antibodies after treatment with pMe-cAMP or Bnz-cAMP and found that the activation of Epac by pMe-cAMP significantly increased the amount of Bim associated with Bcl-2 in cortical neurons 24 h after the treatment (Fig. 5, *A* and *D*). Association of Bim with Bcl2 was also increased 10 h after Epac activation (Fig. 5, *B* and *E*), suggesting that association of Bim with Bcl2 was increased in accordance with increased Bim expression. Activation of PKA by Bnz-cAMP did not promote binding Bcl-2 with Bim even 24 h after treatment (Fig. 5, *H* and *I*).

Because it is already known that Bcl-2 regulates the mitochondrial pathway of apoptosis, we next explored whether pMe-cAMP induced apoptosis through the mitochondrial pathway in cortical neurons. Disruption of mitochondrial transmembrane potential is one of the earliest intracellular events, and such disruption occurs after induction of apoptosis via mitochondria (1). In apoptotic cells, the mitochondrial membrane potential is dissipated, and thus, the Mitocapture dye is dispersed in the cell as green fluorescent monomers detected at 488 nm. We found that Epac activation with pMe-cAMP (50 μM) promoted the disruption of mitochondrial transmembrane potential based on 488-nm-positive (green fluorescence) intensity in cortical neurons (Fig. 5, *J* and *K*). Taken together, these data suggest that stimulation of Epac promotes the binding of Bim to Bcl-2, leading to neuronal apoptosis via the mitochondrial pathway.

Epac-induced Neuronal Apoptosis Is Mediated by Bim—To further confirm the contribution of Bim to Epac-induced apo-

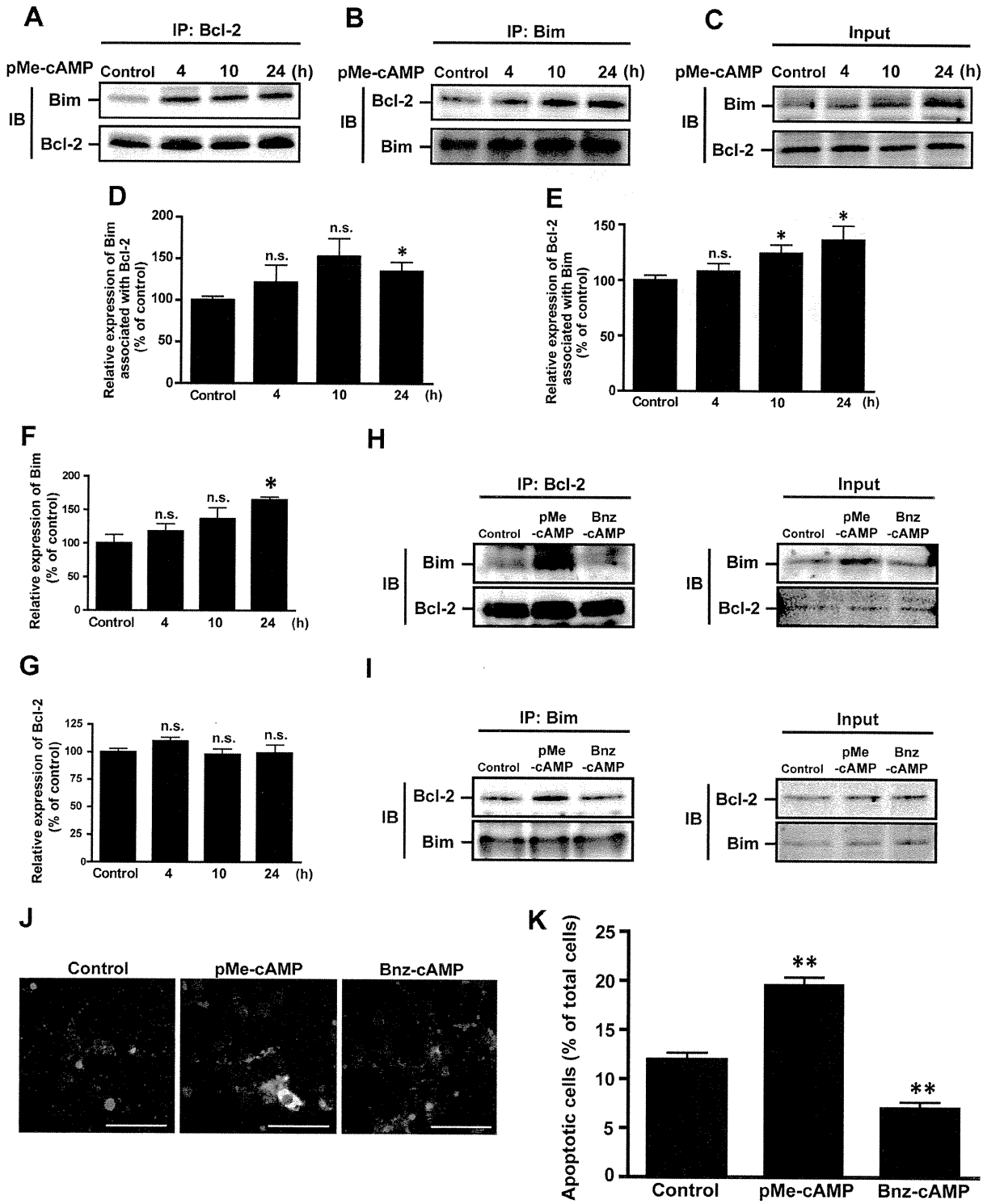

FIGURE 5. **Activation of Epac promoted interaction between Bcl-2 and Bim protein and decreased mitochondrial transmembrane potential in cortical neurons.** *A–C*, a representative immunoblot (*IB*) shows the interaction between Bcl-2 and Bim protein was increased by treatment with pMe-cAMP (50 μM) in a time-dependent manner. *IP*, immunoprecipitate. *D–G*, the pixel intensity of the bands obtained in each experiment was calculated. The results are presented as percentages of the intensity of the corresponding bands in the control experiment. $n = 5$ from 5 independent experiments. *n.s.*, not significant. **, $p < 0.05$ *versus* control. *H* and *I*, interaction of Bim and Bcl-2 in cortical neurons 24 h after incubation with pMe-cAMP (50 μM) or Bnz-cAMP (50 μM) was observed by means of immunoprecipitation with an antibody to Bim or Bcl-2. *J*, the changes in mitochondrial transmembrane potential were detected using the MitoCapture Apoptosis detection kit 48 h after the addition of pMe-cAMP (50 μM) or Bnz-cAMP (50 μM) in cortical neurons. Representative photomicrographs of cortical neurons stained with a cationic dye that fluoresces red in intact cells and green in apoptotic cells are shown. All nuclei were stained with DAPI (*blue*). *Scale bar*, 50 μm. *K*, apoptotic cells were counted, and their incidence was calculated. The results are presented as percentages of the total cell number. $n = 4$; **, $p < 0.01$ *versus* control.

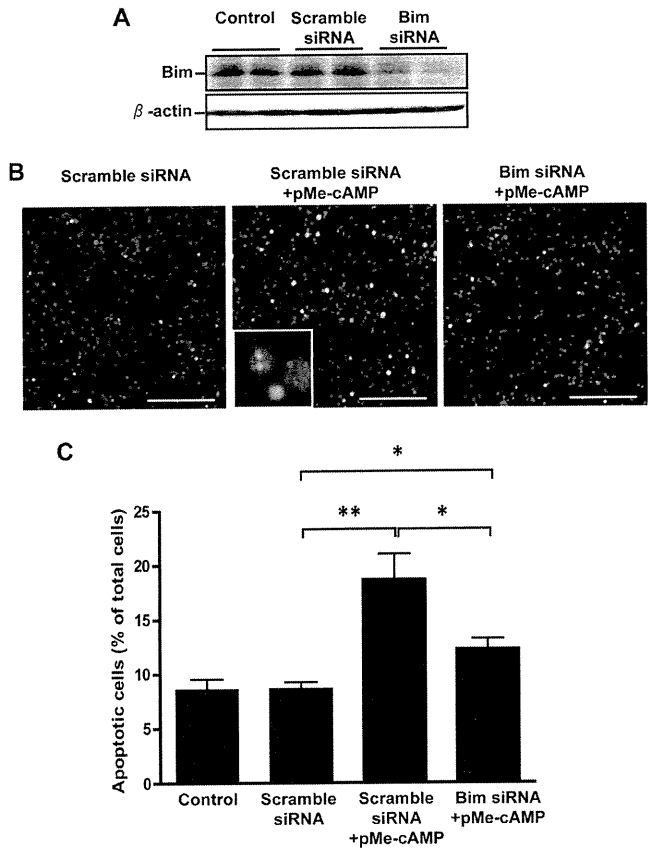

FIGURE 6. **Silencing of Bim attenuated Epac-induced apoptosis in cortical neurons.** *A*, shown is a representative immunoblot of Bim 72 h after transfection of Bim-targeted siRNA or negative siRNA control in cortical neurons. *B*, cortical neurons were transfected with indicated siRNA for 72 h, then treated with pMe-cAMP (50 μM) for 48 h. Apoptotic cells (*green*) were analyzed for TUNEL staining. All nuclei were stained with DAPI (*blue*). *Scale bar*, 100 μm. *C*, TUNEL-positive cells were quantified by counting nuclei in cortical neurons. The results are presented as percentages of the total cell number. $n = 4$; **, $p < 0.01$; *, $p < 0.05$ *versus* scramble siRNA. *n.s.*, not significant.

ptosis is in cortical neurons, we used Bim-targeted siRNA. Changes in Bim protein expression caused by the siRNAs are shown in Fig. 6*A*. When Bim was silenced, the effect of pMe-cAMP on the number of TUNEL-positive cells in cortical neurons became significantly smaller (Fig. 6, *B* and *C*), although Epac-induced apoptosis was not completely abolished. The evidence suggests that enhanced Bim expression via p38 MAPK appears to play an important role in Epac-induced apoptosis in neuronal cells.

Effects of Apoptotic Stimuli on Cortical Neurons of Epac1 KO Mice—Two isoforms of Epac, Epac1 and Epac2, have been previously identified (9) and are known to be activated by pMe-cAMP. In the present study we focused on the role of Epac1, because changes in Epac1 expression have been demonstrated in Alzheimer disease and in neuronal cells (13–15). It has, therefore, been tentatively proposed that Epac inactivation might play a protective role against neuronal apoptosis.

To test this theory, we generated Epac1 KO mice (see "Experimental Procedures" and Fig. 7*A*), which lacked Epac1 expression in neuronal cells as shown by Northern blot analysis (Fig. 7*D*). pMe-cAMP-induced Rap1 activation in Epac1 KO mice was significantly decreased in renal epithelial cells (Fig. 7*E*). Because renal epithelial cells do not express Epac2, this decrease in Rap1 activation most likely mirrors the impact of Epac1 deletion.

Induction of neuronal apoptosis has been well demonstrated in cortical neuronal cells using 3-NP (26, 39) or hydroxyl peroxide (40, 41). Using these pharmacological stressors, we examined whether the induction of apoptosis could be altered in cultured neuronal cells obtained from Epac1 KO mice. Apoptosis induced by hydroxyl peroxide or 3-NP, an irreversible inhibitor of mitochondria complex II, and detected through TUNEL staining was significantly decreased in neuronal cells from Epac1 KO mice (Fig. 8, *A* and *B*). Furthermore, both mRNA and protein expression levels of Bim remained significantly lower in cells from Epac1 KO mice than in those from WT mice (Fig. 8, *C–E*), suggesting that Epac1 deletion plays a protective role against neuronal stresses.

Deletion of Epac1 Attenuates 3-NP-induced Neuronal Apoptosis in Vivo—To examine the effect of Epac1 deletion *in vivo*, we administered 3-NP systemically to intact mice; this is a chemical and pathological way to induce mitochondrial and degenerative disorders *in vivo* (26, 39). We determined the number of apoptotic cells in cortical and striatal regions of Epac1 KO and WT mice through TUNEL staining. We found that 3-NP-induced apoptosis was significantly decreased in both the cortices and the striata of Epac1 KO mice *in vivo* (Fig. 9, *A*, *B*, *D*, and *E*). We confirmed that TUNEL-positive cells were stained with NeuN, a neuron-specific marker (supplemental Fig. 3). Furthermore, the number of cleaved caspase 3-positive cells was significantly increased in WT mice treated with 3-NP and was attenuated in Epac1 KO mice treated with 3-NP (Fig. 9, *A*, *C*, *D*, and *F*).

Taken together, these results reveal that Epac plays an important role in inducing neuronal, but not myocardial, apoptosis. More importantly, its role in this process is different from that of PKA. We found that neuronal apoptosis was, at least partially, mediated by Epac-Bim signaling and that Epac silencing had a protective role against apoptosis *in vivo*. Inhibition of Epac might be considered as a therapeutic strategy for the treatment of neurodegenerative diseases.

DISCUSSION

It is well known that cAMP signaling increases neuronal cell survival and decreases myocardial cell survival. We have demonstrated here that the activation of cAMP signaling does not protect neuronal cells when Epac is selectively activated. Rather, cAMP signaling increased apoptosis in neuronal cells when Epac1 was activated. In myocardial cells, however, Epac activation does not promote apoptosis. To our knowledge this is the first demonstration of the differential role of Epac in apoptosis in neuronal and myocardial cells, both of which are typical post-mitotic cells. The present study suggests that neuronal apoptosis is partly mediated by Epac through increased Bim expression and that the inhibition of Epac signaling plays a protective role in neuronal apoptosis *in vivo*.

The Roles of Epac and PKA in Apoptosis—The effect of cAMP signaling on cell death has been explored in multiple cell types, although most of these studies were conducted before Epac was

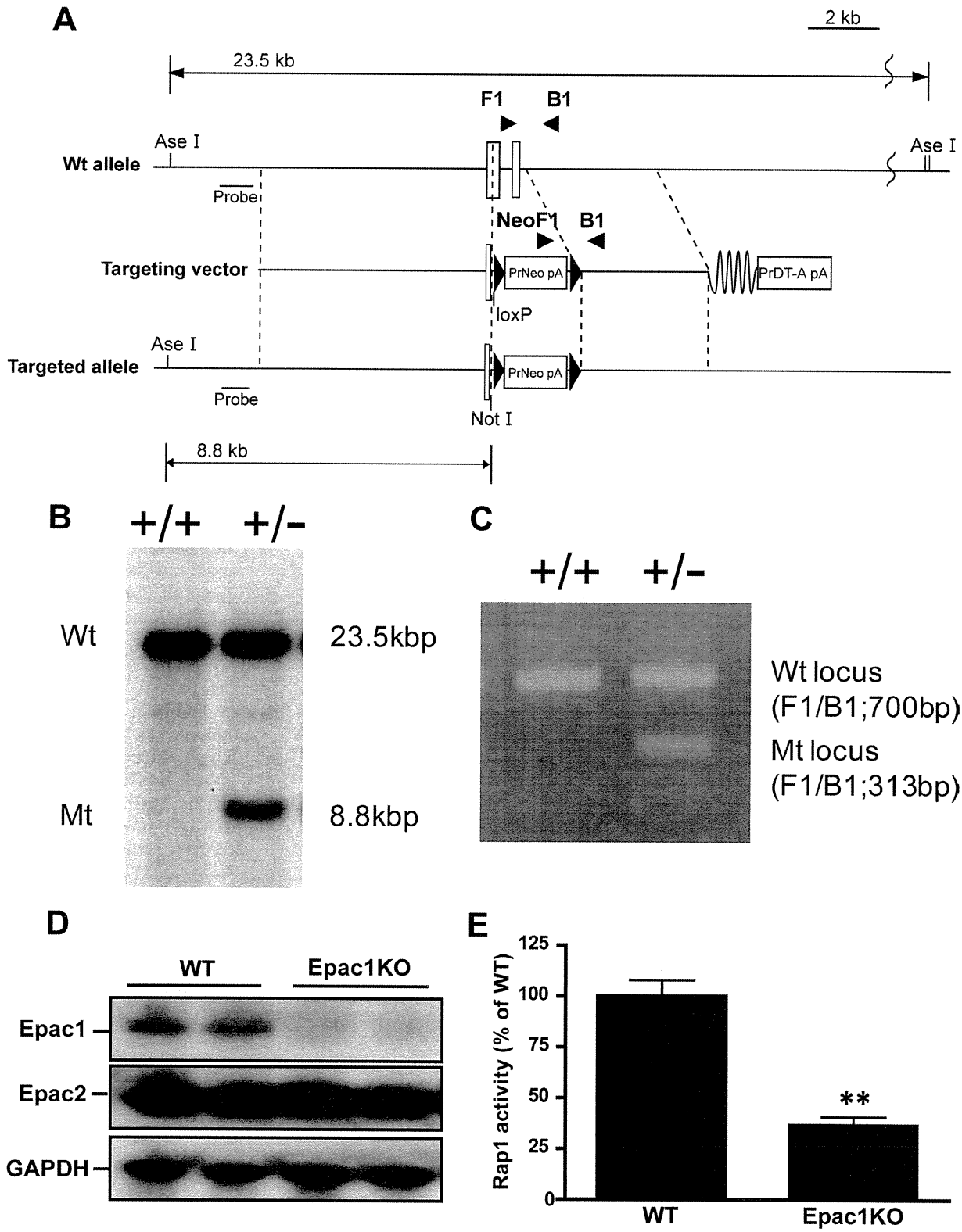

FIGURE 7. **Generation of Epac1 gene-targeted mice.** *A*, targeted disruption of the Epac1 gene is shown. The partial structure of the Epac1 gene (WT) and the resultant mutated allele (Epac1 KO) are shown. The positions of the phosphoglycerate kinase promoter neo cassette (*Neo*) and 5′-probe are indicated. *B*, shown is a Southern blot analysis of targeted embryonic stem cell (*ES*) clones. Genomic DNA from control TT2 ES cells and homologous targeted clones was digested with AseI and Not1 and hybridized with the probe as indicated in *A*. *C*, genotyping mice by PCR is shown. *D*, Northern blot analysis of Epac1, Epac2, and glyceraldehyde-3-phosphate dehydrogenase (*GAPDH*) in the brains of WT and Epac1 KO mice is shown. *E*, Rap1 activation of renal epithelial cells from WT and Epac1 KO mice 15 min after treatment with pMe-cAMP (50 μM) is shown. The data are normalized to total Rap1. $n = 4$; **, $p < 0.01$ *versus* WT mice.